Final Draft
of the original manuscript:

Nazarenko, L.; Bargmann, S.; Stolarski, H.:
Energy-equivalent inhomogeneity approach to analysis of effective properties of nanomaterials with stochastic structure
In: International Journal of Solids and Structures (2015) Elsevier

DOI: 10.1016/j.ijsolstr.2015.01.026

Energy-Equivalent Inhomogeneity Approach to Analysis of Effective Properties of Nano-materials with Stochastic Structure

Lidiia Nazarenko[a,*], Swantje Bargmann[a,b], Henryk Stolarski[c]

[a] Institute of Materials Research, Materials Mechanics, Helmholtz-Zentrum Geesthacht, Germany
[b] Institute of Continuum Mechanics and Material Mechanics, Hamburg University of Technology, Germany
[c] Department of Civil, Environmental and Geo- Engineering, University of Minnesota, 500 Pillsbury Drive S.E., Minneapolis, MN 55455, USA

Abstract

A mathematical model based on the method of conditional moments combined with a new notion of the energy-equivalent inhomogeneity is presented and applied in the investigation of the effective properties of a material with randomly distributed nano-particles. The surface effect is introduced via Gurtin-Murdoch equations describing the properties of the matrix/nano-particle interface. The real system, consisting of the inhomogeneities and their surfaces possessing different properties and, possibly, residual stresses, is replaced by energy-equivalent inhomogeneities with modified bulk properties which incorporate the surface effects. The effective stiffness tensor of the material with so defined equivalent inhomogeneities is determined by the method of conditional moments. Closed-form expressions for the effective moduli of a composite consisting of a matrix and randomly distributed spherical inhomogeneities are derived for both the bulk and the shear moduli. Dependence of those moduli on the radius of nano-particles is included in these expressions exhibiting analytically the nature of the size-dependence in nano-materials. As numerical examples, nanoporous aluminum and nanoporous gold are investigated. The dependence of the normalized bulk and shear moduli of nanoporous aluminum (for two sets of surface properties) on the pore volume fraction (for different radii of nano-pores) and on the radius of nano-pores (for fixed volume fraction of nano-pores) are compared to and discussed in the context of other theoretical predictions. Further, the normalized effective Young's modulus of nanoporous gold as a function of void volume fraction for various ligament radii is analyzed.

Keywords: spherical nanoparticles, composites of stochastic structure, effective properties, Gurtin-Murdoch interface conditions, size dependence, nanoporous metals

1. Introduction

The objective of this work is to investigate effective properties of composites with nanometer-scale randomly dispersed spherical inhomogeneities. They belong to a wider class of materials which, for example, may contain randomly distributed pores, inclusions, cracks etc. of various sizes, shapes and orientations. Some of those materials are increasingly of interest in modern technological applications, and that often includes composites with randomly distributed spherical nano-particles (Kickelbick 2007; Ma and Kim 2011; Wang and Weissmüller 2013; Sarac et al. 2014).

It is commonly known that the conditions at the interface between the matrix and the inhomogeneities impact the overall properties of the composite. A thin layer along the interface between two dissimilar materials typically possesses properties which are different than those

*Corresponding author: e-mail: lidiia.nazarenko@hzg.de, tel.: +49(0) 415287 2605, fax.: +49(0) 415287 42605 (L. Nazarenko).

of the constituent materials on either side of it (Ma and Kim 2011, Tserpes and Silvester 2014). A significant residual interface stresses or interface cracks may be present as well (see, e.g., Gan 2009). The influence of those interface features on the composite's overall properties depends on their kind and their intensities (or magnitude), as well as on some characteristics of the composite itself. Depending on the specific circumstances, they may decrease or increase the stiffness of the composite and appropriate interface models need to be used to capture those effects. If interfacial cracks are present, for example, the composite's overall properties may decrease appreciably - even if the inhomogeneities are well above the nanometer scale (Kim and Mai 1998). On the other hand, changed material properties in a thin layer along the interface, or the residual interface stresses, have been found to meaningfully affect the overall material properties only if the size of the inhomogeneities is in the range of nanometers (see Buryachenko et al. 2005; He and Li 2006; Lim et al. 2006; Wang and Weissmüller 2013; Yang 2004). The quantification of the effects which the changed interface properties have on the overall behavior of random nano-composites is undertaken in this work. The interface model adopted here is that of Gurtin and Murdoch (1975, 1978), whereby the interface is treated as vanishingly thin layer with its own elastic properties (and, possibly, surface tension) coherently connected to the materials on either side. Although not valid universally, this model is adequate for many materials of practical interest and in recent years has been used quite extensively. Several authors modified the known deterministic micromechanical models and, using Gurtin and Murdoch's theory, introduced the surface elasticity and/or surface tension in analysis of random materials on the nanometer scale (see McBride et al. 2011, 2012; Javili et al. 2013 among others).

There are many prior publications addressing the same problem. Those most relevant to the ideas presented in this work are reviewed subsequently. It is important to underscore that this work differs in that the random nature of the analyzed composite is matched by the stochastic nature of the approach used to investigate it. Specifically, the stochastic method of conditional moments (MCM), developed earlier to analyze composites without the interface effects (Khoroshun 1978; Khoroshun et al. 1990, 1992, 1993; Nazarenko et al. 2009), is extended here to include such effects. In fact, the present authors have used a preliminary extension in a previous work of theirs, Nazarenko et al. (2014), but the approach pursued there is too complex to obtain a complete characterization of the composite, but can rather be used to obtain the bulk modulus of the material. In the current work, the MCM is amended in a different way so as to account for the changed interface properties and obtain all properties of the composite. The idea is to, at a specific stage of the development, treat the inhomogeneities and their surfaces with different material properties as one energetic system and replace it by uniform, energy-equivalent inclusions. A similar approach was used in Chen et al. (2007) and Brisard et al. (2010), where the influence of surface stresses on the composite's effective properties are considered as a correction to the properties of the inclusions. Although not explicitly stated in their work (and, possibly, not intended), in fact, the approach of Duan et al. (2005) is also similar in the sense that the surface effects (as shown subsequently for bulk moduli in Section 4) appear only as a modification of the properties of inhomogeneities. As in the case of the previous results obtained using the MCM, closed-form formulas describing the effective properties are obtained also in this work.

The body of literature addressing the issue of surface effects in nano-composites is growing at an increasing rate. The picture gleaned from the literature shows that virtually all of the existing publications employ deterministic techniques, even if analyzing composites with random microstructure. Two basic groups of techniques employed for this purpose can be identified. One is based on various forms of the self-consistent method (Willis 1977), in which a deterministic solution for a single inclusion embedded in a homogeneous medium (Eshelby 1957) is the main ingredient of the techniques, (see Chen et al. 2007; Duan et al.

2005; Sharma and Ganti, 2004, among others). The techniques belonging to the other group invariably employ some kind of computational approach to find elastic fields in the (randomly generated) repeating unit cell, the so-called representative cluster (Mogilevskaya et al. 2010a,b) or in a randomly generated representative volume element (see, e.g., Kushch et al. 2013) , which are then post-processed in various ways to obtain the effective properties of the composite of interest (Kim and Mai 1998; Kanit et al. 2003 among others). Such analysis is computationally very demanding, particularly in the case of realistic three-dimensional problems. In contrast, the statistical approach proposed herein is analytical and leads to the closed-form expressions defining the effective properties of the material.

As mentioned earlier, this work is second in the sequence employing the method of conditional moments, a purely statistical approach, in analysis of surface effects in random nanocomposites. The details of this work are arranged in the following order. To have a self-contained exposition of the material in the next Section some known aspects of the problem are reviewed: the governing equations of elasticity are cast in the form convenient for subsequent use in the context of the MCM, Gurtin-Murdoch description of the interface is inserted, and reference is made to the authors previous results on the subject to justify the present approach. The idea of an energy-equivalent inhomogeneity is discussed in Section 3. It starts with the arguments behind selection of the reference medium in the MCM, which is one of the critical aspects of the approach based on the notion of equivalent inhomogeneity. The description of equivalent inhomogeneity itself, which is the other critical aspect, is included at the end of Section 3. The development of the scalar and tensorial formulas for the effective properties resulting from the proposed approach is presented in Section 4. Sections 5 and 6 are dedicated to the discussion of the numerical results and to general comments on the proposed approach, respectively.

2. Problem statement

2.1 Governing equations

Consider a representative macro-volume V consisting of a matrix with randomly distributed nano-inhomogeneities. Under homogeneous loading, the stresses and strains in the representative volume forms statistically homogeneous random fields satisfying the ergodicity condition. This allows the operation of averaging over a representative volume to be replaced by the operation of the averaging over an ensemble of realizations. Then, the averaged macroscopic stresses $\bar{\boldsymbol{\sigma}}$ and strains $\bar{\boldsymbol{\varepsilon}}$ are related as follows

$$\bar{\boldsymbol{\sigma}} = \mathbf{C}^* : \bar{\boldsymbol{\varepsilon}}, \tag{2.1}$$

where $\mathbf{C}^*$ is the effective stiffness tensor, and the over-bar denotes the operation of the averaging over an ensemble of realizations. The objective of this work is to examine the effects of the properties of constituents, volume fraction, size, shape, orientation, and distribution of inclusions as well as the effects of surface stresses on the overall behavior of the composite, and to determine the effective stiffness tensor as a function of those properties.

For linear elastic materials the problem of finding the effective stiffness tensor outlined in the previous paragraph requires the solution of the following set of equations

- equations of equilibrium:

$$\operatorname{div} \boldsymbol{\sigma}(\mathbf{x}) = \mathbf{0}, \tag{2.2}$$

- Hooke's law:

$$\boldsymbol{\sigma}(\mathbf{x}) = \mathbf{C}(\mathbf{x}) : \boldsymbol{\varepsilon}(\mathbf{x}), \tag{2.3}$$

- linear kinematic relation:

$$\boldsymbol{\varepsilon}(\mathbf{x}) = \mathrm{sym}(\nabla\,\mathbf{u}(\mathbf{x})), \tag{2.4}$$

where **x** is the position vector of a micro-point, i.e, any point in the domain of the composite. They need to be supplemented by the Gurtin-Murdoch equations (see Gurtin and Murdoch, 1975, 1978) describing the kinematic and kinetic compatibility conditions between the matrix and the nano-inhomogeneities at the interface S_I

$$[\![\mathbf{u}(\mathbf{x})]\!]_{S_I} = \mathbf{0}, \qquad [\![\sigma(\mathbf{x})]\!]_{S_I}\cdot\mathbf{n}(\mathbf{x}) + \mathrm{div}_{S_I}\,\boldsymbol{\sigma}_S(\mathbf{x}) = \mathbf{0}. \tag{2.5}$$

In the above formulas $\boldsymbol{\sigma}(\mathbf{x})$ and $\boldsymbol{\varepsilon}(\mathbf{x})$ are the stress and strain tensors, $\mathbf{u}(\mathbf{x})$ is the displacement vector, the fourth-order tensor of elastic constants $\mathbf{C}(\mathbf{x})$ is a random, statistically homogeneous function of coordinates with a finite scale of correlation and linked to the inclusion and to the matrix properties via

$$\mathbf{C}(\mathbf{x}) = \mathbf{C}_1 H(z(\mathbf{x})) + \mathbf{C}_2 H(-z(\mathbf{x})), \tag{2.6}$$

where H is the Heaviside function and $\mathbf{C}_1$ and $\mathbf{C}_2$ denote the values of the tensors of elastic moduli in the inclusions and in the matrix, respectively. The function $z(\mathbf{x})$ is any function satisfying the following requirements:

$$\begin{aligned} &z(\mathbf{x}) > 0, \quad \text{if} \quad \mathbf{x}\in V_1 \\ &z(\mathbf{x}) = 0, \quad \text{if} \quad \mathbf{x}\in S_I, \\ &z(\mathbf{x}) < 0, \quad \text{if} \quad \mathbf{x}\in V_2 \end{aligned} \tag{2.7}$$

where V_1 and V_2 are the domains of the inclusions and the matrix, respectively.

The unit vector $\mathbf{n}$ in Eq. (2.5) is normal to the interface. In the current contribution, it is assumed that at each interface the normal $\mathbf{n}$ points away from the inclusion. The square brackets indicate the jump of the field quantities across the interface, defined as their value on the side towards which the normal $\mathbf{n}$ is pointing minus their value on the side from which it is pointing. The term $\mathrm{div}_{S_I}\,\boldsymbol{\sigma}_S$ denotes the surface divergence of the surface stress tensor $\boldsymbol{\sigma}_S$ (Gurtin and Murdoch, 1978)

$$\boldsymbol{\sigma}_S(\mathbf{x}) = \tau_0\mathbf{I}_S + [\lambda_S + \tau_0]\mathrm{tr}(\boldsymbol{\varepsilon}_S(\mathbf{x}))\,\mathbf{I}_S + 2[\mu_S - \tau_0]\,\boldsymbol{\varepsilon}_S(\mathbf{x}) + \tau_0\nabla_{S_I}\mathbf{u}(\mathbf{x}). \tag{2.8}$$

In the equation above, $\boldsymbol{\varepsilon}_S$ is the interface/surface strain tensor, $\mathbf{I}_S$ represents the identity tensor in the plane tangent to the surface, τ_0 is the magnitude of the deformation-independent surface/interfacial tension (assumed "hydrostatic" and constant in Gurtin-Murdoch model), and λ_S, μ_S are surface Lamé constants.

2.2 General methodology for the proposed approach

Inserting Eq. (2.3) into Eq. (2.2) and accounting for the stress jump across the particle/matrix interface of Eq. (2.5) one obtains

$$\mathrm{div}\,\boldsymbol{\sigma}(\mathbf{x}) = \mathrm{div}(\mathbf{C}(\mathbf{x}):\boldsymbol{\varepsilon}(\mathbf{x})) + [\![\boldsymbol{\sigma}(\mathbf{x})]\!]\cdot\mathbf{n}(\mathbf{x})\,\delta(z(\mathbf{x})) = \mathbf{0}, \qquad z(\mathbf{x}) = \mathbf{0}\big|_{\mathbf{x}\in S_I}. \tag{2.9}$$

Here, $\delta(\bullet)$ is the Dirac delta function, while $z(\mathbf{x})$ is specified in Eq.(2.7). The last term in Eq. (2.9) is interpreted as a body force applied along the interface. In analysis of classical composites with large inhomogeneities, this term is typically neglected as its influence is negligibly small. In the case of nano-inhomogeneities whose curvature radius is small, this term is important, has to be retained in Eq. (2.9) and it's special handling constitutes the essence of the proposed work.

Inserting Eq. (2.4) into Eq. (2.9) and taking into account the second condition in (2.5) yields

$$\mathrm{div}\big(\mathbf{C}(\mathbf{x}) : \mathrm{sym}(\nabla \mathbf{u}(\mathbf{x}))\big) - \delta\big(z(\mathbf{x})\big)\,\mathrm{div}_S\,\boldsymbol{\sigma}_S(\mathbf{x}) = \mathbf{0}\,. \tag{2.10}$$

In the MCM approach the random fields $\mathbf{C}(\mathbf{x})$ and $\mathbf{u}(\mathbf{x})$ are decomposed into fluctuations and averages

$$\mathbf{C}(\mathbf{x}) = \mathbf{C}^0(\mathbf{x}) + \mathbf{C}_c\,, \qquad \mathbf{u}(\mathbf{x}) = \mathbf{u}^0(\mathbf{x}) + \bar{\boldsymbol{\varepsilon}} \cdot \mathbf{x}\,, \tag{2.11}$$

yielding

$$\mathrm{div}\big(\mathbf{C}_c : \mathrm{sym}(\nabla \mathbf{u}^0(\mathbf{x}))\big) + \mathrm{div}\big(\mathbf{C}^0(\mathbf{x}) : \boldsymbol{\varepsilon}(\mathbf{x})\big) - \delta\big(z(\mathbf{x})\big)\,\mathrm{div}_S\,\boldsymbol{\sigma}_S(\mathbf{x}) = \mathbf{0}\,. \tag{2.12}$$

The tensor $\mathbf{C}_c$ (representing the elastic moduli of the so-called reference medium) is constant and its selection determines in many respects the closeness of the calculated values of the effective constants to the true values. The question of the choice of the reference medium tensor is important in the present approach and is discussed in the next section.

The solution of Eq. (2.12) can be formally expressed in terms of Green's function which, in this development, is defined by the following boundary-value problem

$$\mathrm{div}\big(\mathbf{C}_c : \nabla \mathbf{G}(\mathbf{x})\big) + \delta(\mathbf{x})\overset{2}{\mathbf{I}} = \mathbf{0}\,, \qquad \mathbf{G}(\mathbf{x})\big|_{\infty} = \mathbf{0}\,. \tag{2.13}$$

The formula defining the fluctuations in the displacement field within the entire region *V*, described by Eq. (2.12), has the following form (see Nazarenko et al. 2014)

$$\mathbf{u}^0(\mathbf{x}) = \int_{V_y} \mathbf{G}(\mathbf{x}-\mathbf{y}) \cdot \mathrm{div}\big(\mathbf{C}^0(\mathbf{y}) : \boldsymbol{\varepsilon}(\mathbf{y}) - \boldsymbol{\beta}\big)\mathrm{d}V_y - \oint_{S_y} \mathbf{G}(\mathbf{x}-\mathbf{y}) \cdot \mathrm{div}_S\,\boldsymbol{\sigma}_S(\mathbf{y})\,\mathrm{d}S_y\,. \tag{2.14}$$

where $\boldsymbol{\beta}$ is an arbitrary constant. Here, $\delta(\mathbf{x})$ denotes the Dirac delta function and $\overset{2}{\mathbf{I}}$ is the identity tensor of second rank. Expression (2.14) relates the displacement field $\mathbf{u}^0(\mathbf{x})$ to the unknown strain field $\boldsymbol{\varepsilon}(\mathbf{x})$ and the interface values of the displacements which enter the definition of $\boldsymbol{\sigma}_S(\mathbf{x})$. The first integral in Eq. (2.13) is the classical part (Nazarenko et al. 2009), while the second integral represents an additional contribution of surface forces.

The boundary conditions on the surface of the macro-volume are

$$\mathbf{u}^0(\mathbf{x})\big|_S = \mathbf{0}\,. \tag{2.15}$$

The characteristic dimensions of the macro-volumes and macro-surfaces are significantly larger than those of the inclusions. Therefore, in the subsequent development we consider them as infinite and the boundary conditions take the form

$$\mathbf{u}^0(\mathbf{x})\big|_{\infty} = \mathbf{0} \tag{2.16}$$

The linear kinematic relations of Eq. (2.4) combined with Eq. (2.14) and with Gauss' theorem leads to the following stochastically non-linear integral equations for the random strain field (see Nazarenko et al. 2014 for more details)

$$\boldsymbol{\varepsilon}(\mathbf{x}) = \bar{\boldsymbol{\varepsilon}} + \mathbf{K}(\mathbf{x}-\mathbf{y}) * \big[\mathbf{C}^0(\mathbf{y}) : \boldsymbol{\varepsilon}(\mathbf{y})\big] - \mathrm{sym}\left\{\nabla_x \oint_{S_I} \mathbf{G}(\mathbf{x}-\mathbf{y}) \cdot \mathrm{div}_S\,\boldsymbol{\sigma}_S(\mathbf{y})\,\mathrm{d}S_I\right\}. \tag{2.17}$$

The operator $\mathbf{K}(\mathbf{x}-\mathbf{y})$ acts according to

$$\mathbf{K}(\mathbf{x}-\mathbf{y}) * \boldsymbol{\psi}(\mathbf{y}) = \int_V \mathrm{sym}\big(\nabla_x(\nabla_x \mathbf{G}(\mathbf{x}-\mathbf{y}))\big) : \big(\boldsymbol{\psi}(\mathbf{y}) - \bar{\boldsymbol{\psi}}\big)\,\mathrm{d}V_y\,, \tag{2.18}$$

where $\bar{\boldsymbol{\varepsilon}}$ and $\bar{\boldsymbol{\psi}}$ are mean (expectation) values of $\boldsymbol{\varepsilon}(\mathbf{x})$ and $\boldsymbol{\psi}(\mathbf{y})$.

Via $\boldsymbol{\sigma}_S(\mathbf{x})$ and its dependence on $\boldsymbol{\varepsilon}_S$, the surface integral in Eq. (2.17) is ultimately related to strains within the inhomogeneities. Thus, Eq. (2.17) provides a formal and precise basis for calculation of strains and, consequently, their averages. Use of those averages and subsequently calculated stress averages in Eq. (2.1) leads to $\mathbf{C}^*$. This sequence of steps is characteristic of the general methodology used to evaluate the effective properties of composites, including nano-composites.

Remark:

An example of an approach based on such a general methodology is presented in Nazarenko et al. (2014) where Eq. (2.17) was used to directly compute strain averages. To this end the integral equation (2.17) was averaged with respect to the multipoint conditional densities (see Nazarenko et al. 2009; 2014). If the averaging process is limited to two-point approximation, a system of algebraic equations for the strain field averaged over components $\bar{\boldsymbol{\varepsilon}}_\nu$ is obtained in the form

$$\bar{\boldsymbol{\varepsilon}}_\nu = \bar{\boldsymbol{\varepsilon}} + \sum_{k=1}^{2} \mathbf{K}^{\nu k} : \mathbf{C}_k^0 : \bar{\boldsymbol{\varepsilon}}_k + \tilde{\mathbf{K}} : \bar{\boldsymbol{\varepsilon}}_1 + \tau_0 \tilde{\tilde{\mathbf{K}}}, \quad k, \nu \in \{1, 2\}. \tag{2.19}$$

The algebraic operators $\tilde{\mathbf{K}}$ and $\tilde{\tilde{\mathbf{K}}}$ represent influences of the surface effects. These operators were determined in Nazarenko et al. 2014 under the assumption that the surface gradient of displacements present in Eq. (2.8) is negligible and that the surface strains (as well as those in the entire inhomogeneity) represent “isotropic” stretch (or contraction), i.e., the longitudinal strains at the interface (and elsewhere in the nano-inhomogeneities) are identical in all directions. This assumption made it possible to explicitly evaluate operators $\tilde{\mathrm{K}}$ and $\tilde{\tilde{\mathrm{K}}}$ and to account for the contribution of the surface properties to the effective bulk modulus of the composite. However, the shear modulus could not be evaluated in a similar fashion which motivated search for a different approach.

3. Equivalent inclusion

3.1 The method of conditional moments and selection of the reference medium

In this section, arguments for the specific selection of tensor $\mathbf{C}_c$ are provided. To this end, Eq. (2.17) including the surface integral is considered. As the concept of the equivalent inclusion is meant only to provide an alternative way of accounting for the presence of that surface integral, any conclusion regarding the selection of tensor $\mathbf{C}_c$ based on Eq. (2.17) should be adopted in any other approach aimed at inclusion of the surface effects within the approach using MCM.

The integral equation (2.17) is rewritten in the following form

$$\boldsymbol{\varepsilon}^{(1)} = \bar{\boldsymbol{\varepsilon}} + \mathbf{K}\left(\mathbf{x}^{(1)} - \mathbf{x}^{(2)}\right) * \left(\mathbf{C}^{0(2)} : \boldsymbol{\varepsilon}^{(2)}\right) - \operatorname{sym}\left\{\nabla_x \oint_{S_I} \mathbf{G}(\mathbf{x}^{(1)} - \mathbf{x}^{(2)}) \cdot \operatorname{div}_S \boldsymbol{\sigma}_S^{(2)} \, dS_I \right\}, \tag{3.1}$$

where the following abbreviated notation is introduced

$$\boldsymbol{\varepsilon}^{(1)} = \boldsymbol{\varepsilon}\left(\mathbf{x}^{(1)}\right), \quad \boldsymbol{\varepsilon}^{(2)} = \boldsymbol{\varepsilon}\left(\mathbf{x}^{(2)}\right), \quad \boldsymbol{\sigma}_S^{(2)} = \boldsymbol{\sigma}_S(\mathbf{x}^{(2)}), \text{ and } \mathbf{C}^{0(2)} = \mathbf{C}^0\left(\mathbf{x}^{(2)}\right). \tag{3.2}$$

In the MCM approach conditional statistical averaging is performed on Eq. (3.1) with respect to the two-point conditional density $f\left(\boldsymbol{\varepsilon}^{(1)}, \boldsymbol{\varepsilon}^{(2)}, \mathbf{C}^{(2)}\big|_{\nu}^{(1)}\right)$, i.e., the density of strain distributions at the points $\mathbf{x}^{(1)}$, $\mathbf{x}^{(2)}$, and the elasticity moduli at point $\mathbf{x}^{(2)}$ provided that point $\mathbf{x}^{(1)}$ belongs to the ν-th component of the material, $\nu \in \{1, 2\}$. Considering that point $\mathbf{x}^{(2)}$ in the third term on the right-hand side of Eq. (3.1) belongs the inhomogeneity, and recognizing that (under the assumption of homogeneous strains within the inclusions) $\operatorname{div}_S \boldsymbol{\sigma}_S^{(2)}$ can be represented as, cf. Nazarenko at al. (2014),

$$\operatorname{div}_S \boldsymbol{\sigma}_S^{(2)} = \mathbf{M}(\mathbf{x}^{(2)}) : \boldsymbol{\varepsilon}(\mathbf{x}^{(2)}) + 2\kappa\,\tau_0\,\mathbf{n}(\mathbf{x}^{(2)})\,, \tag{3.3}$$

where $\mathbf{M}(\cdot)$ is a rank three tensor, the following system of algebraic equations is obtained

$$\left\langle \boldsymbol{\varepsilon}^{(1)} \middle| {}^{(1)}_{\nu} \right\rangle = \bar{\boldsymbol{\varepsilon}} + \mathbf{K}\left(\mathbf{x}^{(1)} - \mathbf{x}^{(2)}\right) * \sum_{k=1}^{2} \overline{f}\left({}^{(2)}_{k} \middle| {}^{(1)}_{\nu} \right) \left[\mathbf{C}_k^0 : \left\langle \boldsymbol{\varepsilon}^{(2)} \middle| {}^{(2)}_{k}, {}^{(1)}_{\nu} \right\rangle \right] -$$

$$- \sum_{k=1}^{2} \overline{f}\left({}^{(2)}_{k} \middle| {}^{(1)}_{\nu} \right) \operatorname{sym} \left\{ \nabla_x \oint_{S_I} \mathbf{G}(\mathbf{x}^{(1)} - \mathbf{x}^{(2)}) \cdot \left[\mathbf{M}(\mathbf{x}^{(2)}) : \left\langle \boldsymbol{\varepsilon}^{(2)} \middle| {}^{(2)}_{1}, {}^{(1)}_{\nu} \right\rangle + 2\kappa\,\tau_0\,\mathbf{n}(\mathbf{x}^{(2)}) \right] \mathrm{d}S_I \right\}, \quad \nu \in \{1, 2\}, \tag{3.4}$$

Where, with $\mathbf{C}_k$ being the elastic modulus tensor in the k-th component of the nano-composite, $k \in \{1, 2\}$, $\mathbf{C}_k^0$ is defined as

$$\mathbf{C}_k^0 = \mathbf{C}_k - \mathbf{C}_c\,. \tag{3.5}$$

The function $\overline{f}\left({}^{(2)}_{k} \middle| {}^{(1)}_{\nu} \right)$ denotes the probability that the point $\mathbf{x}^{(2)}$ belongs to the k-th component, provided the point $\mathbf{x}^{(1)}$ belongs to the ν-th component. $\left\langle \boldsymbol{\varepsilon}^{(2)} \middle| {}^{(2)}_{k}, {}^{(1)}_{\nu} \right\rangle$ is the expectation value of the strain tensor at $\mathbf{x}^{(2)}$, provided that $\mathbf{x}^{(2)}$ and $\mathbf{x}^{(1)}$ belong to the k-th component and to the ν-th component, respectively.

For the system of Eq. (3.4) to be completely defined, the two-point conditional moment $\left\langle \boldsymbol{\varepsilon}^{(2)} \middle| {}^{(2)}_{k}, {}^{(1)}_{\nu} \right\rangle$ must be determined. For this purpose, Eq. (3.1) is averaged again, this time over the three-point conditional density $f\left(\boldsymbol{\varepsilon}^{(1)}, \boldsymbol{\varepsilon}^{(2)}, \mathbf{C}^{(2)} \middle| {}^{(3)}_{k}, {}^{(1)}_{\nu} \right)$ to obtain the following system of algebraic equations

$$\left\langle \boldsymbol{\varepsilon}^{(1)} \middle| {}^{(1)}_{\nu}, {}^{(3)}_{k} \right\rangle = \bar{\boldsymbol{\varepsilon}} + \mathbf{K}\left(\mathbf{x}^{(1)} - \mathbf{x}^{(2)}\right) * \sum_{\rho=1}^{2} \overline{f}\left({}^{(2)}_{\rho} \middle| {}^{(1)}_{\nu}, {}^{(3)}_{k} \right) \left[\mathbf{C}_\rho^0 : \left\langle \boldsymbol{\varepsilon}^{(2)} \middle| {}^{(2)}_{\rho}, {}^{(1)}_{\nu}, {}^{(3)}_{k} \right\rangle \right]$$

$$- \sum_{k=1}^{2} \overline{f}\left({}^{(2)}_{\rho} \middle| {}^{(1)}_{\nu}, {}^{(3)}_{k} \right) \operatorname{sym} \left\{ \nabla_x \oint_{S_I} \mathbf{G}(\mathbf{x}^{(1)} - \mathbf{x}^{(2)}) \cdot \left[\mathbf{M}(\mathbf{x}^{(2)}) : \left\langle \boldsymbol{\varepsilon}^{(2)} \middle| {}^{(2)}_{1}, {}^{(1)}_{\nu}, {}^{(3)}_{k} \right\rangle + 2\kappa\,\tau_0\,\mathbf{n}(\mathbf{x}^{(2)}) \right] \mathrm{d}S_I \right\}, \quad k, \nu, \rho \in \{1, 2\}. \tag{3.6}$$

By continuing this process, one obtains an infinite system of equations defining the conditional moments

$$\left\langle \boldsymbol{\varepsilon}^{(1)} \middle| {}^{(1)}_{\nu_1} \right\rangle, \quad \left\langle \boldsymbol{\varepsilon}^{(1)} \middle| {}^{(1)}_{\nu_1}, {}^{(2)}_{\nu_2} \right\rangle, \quad \left\langle \boldsymbol{\varepsilon}^{(1)} \middle| {}^{(1)}_{\nu_1}, {}^{(2)}_{\nu_2}, \ldots, {}^{(i)}_{\nu_i} \right\rangle, \quad \nu_1, \nu_2, \cdots \in \{1, 2\}. \tag{3.7}$$

To determine that system, it is necessary to specify the conditional multipoint probability functions

$$\overline{f}\left({}^{(2)}_{k} \middle| {}^{(1)}_{\nu_1} \right), \quad \overline{f}\left({}^{(2)}_{k} \middle| {}^{(1)}_{\nu_1}, {}^{(3)}_{\nu_2} \right), \quad \cdots, \quad \overline{f}\left({}^{(2)}_{k} \middle| {}^{(1)}_{\nu_1}, {}^{(3)}_{\nu_2}, \ldots, {}^{(i)}_{\nu_i}, \ldots \right), \tag{3.8}$$

which completely characterize shape, orientation and distribution of inhomogeneities.

If the infinite system just described could be solved, the resulting conditional moments of Eq. (3.7) would completely and exactly characterize the analyzed nano-composite. In reality, the process of constructing successive equations of the problem has to be terminated at some step. However, this requires additional conditions to close the truncated system of equations. To this end, one can take, for instance, one of the following conditions

$$\left\langle \boldsymbol{\varepsilon}^{(1)} \middle| {}^{(1)}_{\nu_1}, {}^{(2)}_{\nu_2}, \ldots, {}^{(i)}_{\nu_i} \right\rangle = 0 \ , \ \left\langle \boldsymbol{\varepsilon}^{(1)} \middle| {}^{(1)}_{\nu_1}, {}^{(2)}_{\nu_2}, \ldots, {}^{(i)}_{\nu_i} \right\rangle = \bar{\boldsymbol{\varepsilon}} \ , \ \left\langle \boldsymbol{\varepsilon}^{(1)} \middle| {}^{(1)}_{\nu_1}, {}^{(2)}_{\nu_2}, \ldots, {}^{(i)}_{\nu_i} \right\rangle = \left\langle \boldsymbol{\varepsilon}^{(1)} \middle| {}^{(1)}_{\nu_1} \right\rangle . \tag{3.9}$$

In this work, a two-point approximation is used and the closure of the system is achieved by imposing the condition

$$\left\langle \boldsymbol{\varepsilon}^{(1)} \middle| {}^{(1)}_{\nu_1}, {}^{(2)}_{\nu_2}, \ldots, {}^{(i)}_{\nu_i} \right\rangle = \left\langle \boldsymbol{\varepsilon}^{(1)} \middle| {}^{(1)}_{\nu_1} \right\rangle , \tag{3.10}$$

implying that the strain fluctuations within each component are neglected and requiring only the two-point conditional probabilities $\overline{f}\left({}^{(2)}_{k} \middle| {}^{(1)}_{\nu} \right)$. With this specification it is sufficient to consider only Eq. (3.4) and the additional condition (3.10). In this case, the following system of algebraic equations in terms of component-average strains results

$$\begin{aligned} \bar{\boldsymbol{\varepsilon}}_{\nu} &= \bar{\boldsymbol{\varepsilon}} + \mathbf{K}\left(\mathbf{x}^{(1)} - \mathbf{x}^{(2)}\right) * \sum_{k=1}^{2} p_{\nu k}\left(\mathbf{x}^{(1)} - \mathbf{x}^{(2)}\right)\left[\mathbf{C}_k^0 : \bar{\boldsymbol{\varepsilon}}_k\right] - \\ &- \sum_{k=1}^{2} p_{\nu k}\left(\mathbf{x}^{(1)} - \mathbf{x}^{(2)}\right) \operatorname{sym}\left\{ \nabla_x \oint_{S_I} \mathbf{G}(\mathbf{x}^{(1)} - \mathbf{x}^{(2)}) \cdot \left[\mathbf{M}(\mathbf{x}^{(2)}) : \bar{\boldsymbol{\varepsilon}}_1 + 2\kappa\tau_0\, \mathbf{n}(\mathbf{x}^{(2)})\right] \mathrm{d}S_I \right\}, \end{aligned} \tag{3.11}$$

where

$$\bar{\boldsymbol{\varepsilon}}_{\nu} = \left\langle \boldsymbol{\varepsilon}^{(1)} \middle| {}^{(1)}_{\nu} \right\rangle , \quad p_{\nu k}\left(\mathbf{x}^{(1)} - \mathbf{x}^{(2)}\right) = \overline{f}\left({}^{(2)}_{k} \middle| {}^{(1)}_{\nu} \right). \tag{3.12}$$

Taking into account that

$$\sum_{k=1}^{2} p_{\nu k}\left(\mathbf{x}^{(1)} - \mathbf{x}^{(2)}\right) = 1 , \tag{3.13}$$

one obtains (see Nazarenko et al. 2014)

$$\begin{aligned} \bar{\boldsymbol{\varepsilon}}_{\nu} &= \bar{\boldsymbol{\varepsilon}} + \mathbf{K}\left(\mathbf{x}^{(1)} - \mathbf{x}^{(2)}\right) * \sum_{k=1}^{2} p_{\nu k}\left(\mathbf{x}^{(1)} - \mathbf{x}^{(2)}\right)\left[\mathbf{C}_k^0 : \bar{\boldsymbol{\varepsilon}}_k\right] \\ &+ \operatorname{sym}\left\{ \nabla_x \oint_{S_I} \mathbf{G}(\mathbf{x}^{(2)}) \cdot \mathbf{M}(\mathbf{x}^{(2)})\, \mathrm{d}S_I : \bar{\boldsymbol{\varepsilon}}_1 \right\} + 2\kappa\tau_0 \left(\mathbf{C}_c\right)^{-1} : \mathbf{S} : \overset{2}{\mathbf{I}} , \end{aligned} \tag{3.14}$$

where κ is the mean curvature of the inhomogeneities (i.e., the curvature of the spheres in the present case with an appropriate sign, depending on the orientation of vector $\mathbf{n}$) and $\mathbf{S}$ is the classical Eshelby tensor.

Eq. (3.14) is rewritten as follows

$$\bar{\boldsymbol{\varepsilon}}_{\nu} = \bar{\boldsymbol{\varepsilon}} + \sum_{k=1}^{2} \mathbf{K}^{\nu k} : \mathbf{C}_k^0 : \bar{\boldsymbol{\varepsilon}}_k + \tilde{\mathbf{K}} : \bar{\boldsymbol{\varepsilon}}_1 + 2\kappa\tau_0 \left(\mathbf{C}_c\right)^{-1} : \mathbf{S} : \overset{2}{\mathbf{I}} \ , \tag{3.15}$$

where

$$\mathbf{K}^{\nu k} = \mathbf{K}\left(\mathbf{x}^{(1)} - \mathbf{x}^{(2)}\right) * p_{\nu k}\left(\mathbf{x}^{(1)} - \mathbf{x}^{(2)}\right), \quad \tilde{\mathbf{K}} = \operatorname{sym}\left\{ \nabla_x \oint_{S_I} \mathbf{G}(\mathbf{x}^{(2)}) \cdot \mathbf{M}(\mathbf{x}^{(2)})\, \mathrm{d}S_I \right\}. \tag{3.16}$$

In order to evaluate Eq. (3.15) we specify the two-point conditional probabilities $p_{\nu k}\left(\mathbf{x}^{(1)} - \mathbf{x}^{(2)}\right)$, which characterize the shape and the arrangement of inhomogeneities, construct the tensor of elastic moduli of a reference body $\mathbf{C}_c$ and determine averaged integral operators $\mathbf{K}^{\nu k}$ and $\tilde{\mathbf{K}}$ involving the Green's function $\mathbf{G}(\mathbf{x})$ and tensor $\mathbf{M}(\mathbf{x}^{(2)})$ defined in Eq. (3.3).

An important issue is the selection of the reference medium represented by tensor $\mathbf{C}_c$. It can be chosen in a number of different ways. Each choice may lead to a different result and with this it also determines in many respects the accuracy of the obtained solution. It has been shown in the existing literature (see Khoroshun 1978; Khoroshun et al. 1993), where the choices for $\mathbf{C}_c$ have been discussed without accounting for surface effect, that it is expedient to take $\mathbf{C}_c$ as follows:

$$\mathbf{C}_c = \begin{cases} \overline{\mathbf{C}}, & \text{if} \quad \mathbf{C}_1 \le \mathbf{C}_2 \\ \overline{\overline{\mathbf{C}}}, & \text{if} \quad \mathbf{C}_1 \ge \mathbf{C}_2 \end{cases}, \tag{3.17}$$

with $\overline{\mathbf{C}} = c_1\mathbf{C}_1 + c_2\mathbf{C}_2$ and $\overline{\overline{\mathbf{C}}} = \left[c_1\mathbf{C}_1^{-1} + c_2\mathbf{C}_2^{-1}\right]^{-1}$, where c_1 and $c_2 = 1 - c_1$ denote the volume fractions of the inclusions and of the matrix, respectively, i.e., $c_1 = V_1/[V_1 + V_2]$.

First, to justify the choice made in Eq. (3.17), materials without surface effects are considered. In Eq. (3.11), the tensor $\mathbf{C}_k^0$, dependent on $\mathbf{C}_c$, is present as a multiplier of the component averaged strains only because of restricting the method to two-point approximation. In Eq. (3.6), the tensor $\mathbf{C}_\rho^0$ is multiplied by three-point conditional moments $\left\langle \boldsymbol{\varepsilon}^{(2)} \middle|_{\rho}^{(2)},_{\nu}^{(1)},_{k}^{(3)} \right\rangle$ which in Eq. (3.11) is replaced by the component-averaged strains if the approximation expressed in Eq. (3.10) is introduced. Such approximation introduces errors which, as discussed in Khoroshun (1978) and Khoroshun et al. (1993), are minimized if the selected tensor $\mathbf{C}_c$ is as close to the effective properties of the analyzed material as possible. A good choice is that the tensor of elastic moduli of the reference body $\mathbf{C}_c$ in Eq. (3.17) be selected as the Reuss estimate ($\overline{\overline{\mathbf{C}}}$) or the Voigt estimate ($\overline{\mathbf{C}}$), depending on whether the inhomogeneities are stiff ($\mathbf{C}_1 \ge \mathbf{C}_2$) or soft ($\mathbf{C}_1 \le \mathbf{C}_2$), respectively (see Khoroshun 1978; Khoroshun et al. 1993). As a consequence, $\mathbf{C}_c$ is described by a closed-form expression containing the data characterizing the analyzed material[1] and the proposed approach yields closed-form formulas for the composite's effective properties.

Turning to materials with surface effects the issue of selecting $\mathbf{C}_c$ cannot be resolved in equally definite way. However, the following arguments can be provided to support the choice of $\mathbf{C}_c$ expressed in Eq. (3.17) also in the case of those materials. First, for realistic materials the contribution of the properties of the matrix and inhomogeneities to the effective stiffness tensor is considerably larger than the contribution of the surface effects (which is only a correction to the solution of bulk elasticity equations) even for small radius of nanoparticles. Therefore, the accurate capture of the classical part of the solution for the effective properties is decisive in the analysis. Consequently, it is logical to retain the same value of $\mathbf{C}_c$ as in the classical analysis. Second, the importance of the fluctuations $\mathbf{C}^0$ in elastic constants (consequently the magnitude of the error associated with the approach) are magnified, if the moments of higher order multiplying those fluctuations are replaced by moments of lower order, as done in transition from Eq. (3.4) to Eq. (3.11). However, $\mathbf{C}^0$ – which results from $\mathbf{C}_c$ selected so as to capture contribution of the matrix and inhomogeneities in the best possible way – is not included as a multiplier of the component averaged strains in the third term of the right-hand side of Eqs. (3.4) and (3.6), containing two- and three-point conditional moments. Thus, while departure from Eq. (3.17) in selection of $\mathbf{C}_c$ would lead to some small changes in the part of Eq. (3.11) related to surface effects (and containing $\mathbf{C}_c$ through

[1] As shown in (Khoroshun 1978), in the two limiting cases of $\mathbf{C}_c = 0$ or $\mathbf{C}_c = \infty$, the Reuss and the Voigt bounds result from Eq. (3.11), respectively. On the other hand, by assuming $\mathbf{C}_c$ to be equal the maximum or minimum rigidities, one arrives at the upper and lower Hashin-Shtrikman bounds (Hashin and Shtrikman 1963).

its presence in the Green's function), changes in $\mathbf{C}^0$, associated with selection of $\mathbf{C}_c$ different that one based on Eq. (3.17), is certain to result in much more significant negative effects associated with the matrix and inhomogeneities (containing $\mathbf{C}^0$). As a result, the overall solution might be less accurate.

3.2 Energy-equivalent inclusion

The way to handle the surface effects outlined in the preceding sections is rigorous and constitutes the best alternative within the context of MCM. However, determination of tensor $\mathbf{M}(\mathbf{x}^{(2)})$ and evaluation of the averaged integral operator $\tilde{\mathbf{K}}$ is a rather complex problem for the case of arbitrary loading – only the effective bulk modulus could be determined that way in Nazarenko et al. (2014). To circumvent those difficulties, we propose to account for the contribution of the surface integral in Eq. (3.14) in a different, albeit approximate way. To this end, the effects of the surface integral in Eq. (3.14), de facto the effects associated with the surfaces of the inhomogeneities, are "added" to the effects of the inhomogeneities. It is achieved by requiring that the elastic energy of the uniformly deforming inhomogeneity is augmented by the energy of its surface deforming coherently with it. Effectively, this approach adds an additional part to the inhomogeneity's stiffness tensor, resulting in what we refer to as the energy-equivalent inhomogeneity. Consequently, this is a different way of accounting for the contribution represented by the surface integral.

We consider a single inclusion whose surface is characterized by an independent set of elastic parameters. It is further supposed that the strain tensor representing deformation of the inclusion is constant $\bar{\boldsymbol{\varepsilon}}_1$. The elastic energy of this system is

$$\mathbf{E} = \frac{1}{2} V_I (\bar{\boldsymbol{\varepsilon}}_1 : \mathbf{C}_1 : \bar{\boldsymbol{\varepsilon}}_1) + \frac{1}{2} \oint_{S_I} \boldsymbol{\varepsilon}_S : \mathbf{C}_S : \boldsymbol{\varepsilon}_S \, \mathrm{d}S_I \,, \tag{3.18}$$

where $\boldsymbol{\varepsilon}_S$ is the tensor of the surface strains compatible with $\bar{\boldsymbol{\varepsilon}}_1$, $\mathbf{C}_1$ is the isotropic rank four tensor of elastic moduli of the inclusion

$$\mathbf{C}_1 = 2\mu_1 \overset{4}{\mathbf{I}} + \lambda_1 \overset{2}{\mathbf{I}} \otimes \overset{2}{\mathbf{I}} \,, \tag{3.19}$$

with Lamé constants λ_1, and μ_1, $\overset{4}{\mathbf{I}}$ is the rank four identity tensors; $\mathbf{C}_S$ in Eq. (3.18) is the tensor of surface isotropic elasticity with Lame constants $\bar{\lambda}_S$ and $\bar{\mu}_S$

$$\mathbf{C}_S = 2\bar{\mu}_S \overset{4}{\mathbf{I}}_S + \bar{\lambda}_S \overset{2}{\mathbf{I}}_S \otimes \overset{2}{\mathbf{I}}_S \,, \tag{3.20}$$

where $\bar{\lambda}_S = \lambda_S + \tau_0$, $\bar{\mu}_S = \mu_S - \tau_0$, cf. Eq. (2.8) , $\overset{2}{\mathbf{I}}_S$ and $\overset{4}{\mathbf{I}}_S$ are the rank two and rank four surface identity tensors.

Given that the surface strains $\boldsymbol{\varepsilon}_S$ are related to the strains within the inhomogeneity $\bar{\boldsymbol{\varepsilon}}_1$, the sum of the bulk and surface energies present in Eq. (3.18) are expressed by introducing a single tensor $\tilde{\mathbf{C}}_1$

$$\mathbf{E} = \frac{1}{2} V \left[\bar{\boldsymbol{\varepsilon}}_1 : \tilde{\mathbf{C}}_1 : \bar{\boldsymbol{\varepsilon}}_1 \right], \tag{3.21}$$

which is the tensor of the effective elastic moduli of the energy-equivalent inhomogeneity.

As shown in Appendix A, the surface part of the elastic energy in Eq. (3.18) can be equivalently expressed as

$$\oint_{S_I} \boldsymbol{\varepsilon}_S : \mathbf{C}_S : \boldsymbol{\varepsilon}_S \,\mathrm{d}S_I = \bar{\boldsymbol{\varepsilon}}_1 : \oint_{S_I} \left[2\bar{\mu}_S \overset{4}{\mathbf{I}}_S + \bar{\lambda}_S \overset{2}{\mathbf{I}}_S \otimes \overset{2}{\mathbf{I}}_S \right] \mathrm{d}S_I : \bar{\boldsymbol{\varepsilon}}_1 , \tag{3.22}$$

which, combined with Eqs. (3.18) and (3.21) (see Appendix A Eq. (A.13)), yields

$$\tilde{\mathbf{C}}_1 = \mathbf{C}_1 + \hat{\mathbf{C}} , \tag{3.23a}$$

where

$$\hat{\mathbf{C}} = \frac{1}{V_I} \oint_{S_I} \left[2\bar{\mu}_S \overset{4}{\mathbf{I}}_S + \bar{\lambda}_S \overset{2}{\mathbf{I}}_S \otimes \overset{2}{\mathbf{I}}_S \right] \mathrm{d}S_I . \tag{3.23b}$$

The above development holds for arbitrary shape of the inhomogeneities, but it is valid only if their deformations are uniform. In this contribution, spherical inclusions of radius R_0 are considered. In this case, one obtains the stiffness tensor of equivalent inclusions $\tilde{\mathbf{C}}_1$

$$\tilde{\mathbf{C}}_1 = 2[\mu_1 + \hat{\mu}_S]\overset{4}{\mathbf{I}} + [\lambda_1 + \hat{\lambda}_S]\overset{2}{\mathbf{I}} \otimes \overset{2}{\mathbf{I}} , \tag{3.24}$$

with (see Appendix A, Eq. (A.24))

$$\hat{\lambda}_S = \frac{2}{5R_0}\left[\bar{\mu}_S + 3\bar{\lambda}_S\right], \quad \hat{\mu}_S = \frac{1}{5R_0}\left[7\bar{\mu}_S + \bar{\lambda}_S\right]. \tag{3.25}$$

Following the explanation at the beginning of this section, the evaluation of the effective properties of a nano-material by the method proposed here starts with the use of Eq. (3.17) to determine the tensor $\mathbf{C}_c$. The method of conditional moments is then employed to evaluate the effective properties of the material as if no surface effect existed, but with $\mathbf{C}_1$ replaced by $\tilde{\mathbf{C}}_1$ whenever properties of the inhomogeneities appear independently of $\mathbf{C}_c$.

The following comments may be helpful to further elucidate the proposed approach:

1. Evaluation of $\tilde{\mathbf{C}}_1$ based on the assumption that the strains within the inhomogeneity are constant is in particular agreement with the method of conditional moments restricted to the two-point approximation. This restriction effectively means that the strain fluctuations within the inhomogeneities are neglected.
2. One theoretically possible way to solve the problem of effective constants for multi-constituent elastic materials with surface effects may be based on minimization of the total potential energy of the system. Its elastic part would be the sum of the elastic energies of all of its constituents, and one of them would be the energy associated with the matrix/inhomogeneities interfaces. Although the approach adopted here is different, the presence of the surface strain energy in the potential energy approach would be exactly equivalent to the presence of the surface integral in Eq. (2.14) used here (and in all surface integrals present in the subsequent equations, resulting from Eq. (2.14)). Furthermore, minimization of the potential energy approach can be used to obtain solutions under all kinds of approximating assumptions. That includes a possibility to obtain an approximate solution based on the assumption that the strains within the inhomogeneities are constant. The technique proposed here can then be seen as a combination of two techniques: the method of conditional moments to solve the overall problem of effective constants and the energy approach to include the surface effects by modifying the material constants of the inhomogeneities. Its very valuable attribute is that it eliminates the need to contend with difficult to handle surface integral discussed in the preceding sections.

4. Effective properties

4.1 Algebraic operators resulting from the equivalent inclusion approach in combination with the MCM

In accord with the preceding development, Eq. (3.15) is rewritten in the following form

$$\bar{\boldsymbol{\varepsilon}}_\nu = \bar{\boldsymbol{\varepsilon}} + K^{\nu 1} : \tilde{\mathbf{C}}_1^0 : \bar{\boldsymbol{\varepsilon}}_1 + K^{\nu 2} : \mathbf{C}_2^0 : \bar{\boldsymbol{\varepsilon}}_2 + 2\kappa\,\tau_0 \left(\mathbf{C}_c\right)^{-1} : \mathbf{S} : \overset{2}{\mathbf{I}} \,, \tag{4.1}$$

where the third term in the right-hand side of Eq. (3.15) $\tilde{\mathbf{K}} : \bar{\boldsymbol{\varepsilon}}_1$, resulting from the surface integral and representing surface elasticity, has been incorporated in the second term on the right-hand side of the above equation

$$\tilde{\mathbf{C}}_1^0 = \tilde{\mathbf{C}}_1 - \mathbf{C}_c \,. \tag{4.2}$$

Tensor $\mathbf{C}_c$ is selected in accordance with Eq. (3.17), and the algebraic operator $\mathbf{K}^{\nu k}$ is defined in Eq. (3.16$_1$) as averaged integral operator involving Green's function for infinite medium and the transition probabilities $p_{\nu k}(\mathbf{x})$ of Eq. (3.12). These probabilities can be represented as (Khoroshun et al. 1993)

$$p_{\nu k}(\mathbf{x}) = c_k + \left[\delta_{\nu k} - c_k\right]\Phi(\mathbf{x}) \,, \tag{4.3}$$

where $\Phi(\mathbf{x})$ is a correlation function which only depends on the distance between points for a composite with randomly distributed spherical inclusions of radius R_0. It can be specified on the basis of probability theory and, as shown in Khoroshun et al. (1993); Nazarenko et al. (2009), has the following form

$$\Phi(\mathbf{x}) = \exp\left(-\frac{8}{\pi^2 c_2 R_0}\sqrt{x_1^2 + x_2^2 + x_3^2}\right) . \tag{4.4}$$

Taking into account Eq. (4.4) the algebraic operator $\mathbf{K}^{\nu k}$ can be represented by (Khoroshun et al. (1993); Nazarenko et al. (2014))

$$\mathbf{K}^{\nu k} = \left[\delta_{\nu k} - c_k\right] \mathbf{L} \,, \tag{4.5}$$

where $\mathbf{L}$ is an isotropic rank four tensor (classical Hill tensor, see Mura 1987). It is determined in terms of two scalars a and b

$$\mathbf{L} = 2b\overset{4}{\mathbf{I}} + a\overset{2}{\mathbf{I}} \otimes \overset{2}{\mathbf{I}} \,, \tag{4.6}$$

with

$$a = \frac{\lambda_c + \mu_c}{15\mu_c[\lambda_c + 2\mu_c]} , \quad b = -\frac{3\lambda_c + 8\mu_c}{30\mu_c[\lambda_c + 2\mu_c]} , \tag{4.7}$$

and with λ_c, μ_c being the Lamé constants of the reference medium (Khoroshun et al. 1993).

Taking into account Eq. (4.5), the system of linear algebraic equations (4.1) reads

$$\bar{\boldsymbol{\varepsilon}}_1 = \bar{\boldsymbol{\varepsilon}} + c_2 \mathbf{L} : \left[\tilde{\mathbf{C}}_1^0 : \bar{\boldsymbol{\varepsilon}}_1 - \mathbf{C}_2^0 : \bar{\boldsymbol{\varepsilon}}_2\right] + 2\kappa\,\tau_0\, \mathbf{C}_c^{-1} : \mathbf{S} : \overset{2}{\mathbf{I}} \,. \tag{4.8}$$

This last equation can be simplified using the fact that $\kappa = -1/R_0$ for spheres, where R_0 is their radius (Nazarenko et al. 2014)[2]. Furthermore, it is noted that an isotropic rank four tensor $\mathbf{C}_c$ can be written in terms of Lamé constants

$$\mathbf{C}_c = 2\mu_c \overset{4}{\mathbf{I}} + \lambda_c \overset{2}{\mathbf{I}} \otimes \overset{2}{\mathbf{I}} \,. \tag{4.9}$$

Accounting for Eq. (B.3) the following relation results:

---

[2] The minus sign is due to the assumption that the vector $\mathbf{n}$ normal to the interface is pointing away from the inhomogeneities.

$$\mathbf{C}_c^{-1} : \overset{2}{\mathbf{I}} = \frac{1}{3K_c} \overset{2}{\mathbf{I}}, \tag{4.10}$$

in which K_c is the bulk modulus of the reference medium. Noting that for isotropic spherical inclusions (see Mura 1987) $\mathbf{S} : \overset{2}{\mathbf{I}} = \frac{1+\nu_c}{3[1-\nu_c]} \overset{2}{\mathbf{I}}$ and inserting Eq. (4.9), and Eq. (4.10) into Eq. (4.8), we can eliminate $\bar{\boldsymbol{\varepsilon}}_2$ from Eq. (4.8) to obtain

$$\bar{\boldsymbol{\varepsilon}}_1 = \left[\overset{4}{\mathbf{I}} - \mathbf{L} : \mathbf{C}_2^0 \right] : \bar{\boldsymbol{\varepsilon}} + \mathbf{L} : \tilde{\mathbf{C}}' : \bar{\boldsymbol{\varepsilon}}_1 - \frac{2\tau_0}{9R_0 K_c} \left[\frac{1+\nu_c}{1-\nu_c} \right] \overset{2}{\mathbf{I}}, \tag{4.11}$$

where ν_c is the Poisson's ratio of the reference medium and

$$\tilde{\mathbf{C}}' = \tilde{\mathbf{C}}_4 - \mathbf{C}_c, \quad \tilde{\mathbf{C}}_4 = c_1 \mathbf{C}_2 + c_2 \tilde{\mathbf{C}}_1 . \tag{4.12}$$

The new tensors $\tilde{\mathbf{C}}'$ and $\tilde{\mathbf{C}}_4$ defined in the above equation are isotropic, can be characterized by two Lame constants $\tilde{K}'$, $\tilde{\mu}'$ and $\tilde{K}_4$, $\tilde{\mu}_4$, respectively, and depend on the volume fractions of the composite's constituents.

4.2 Tensor form of effective moduli

Using the relationships for macro stresses $\bar{\boldsymbol{\sigma}} = c_1 \tilde{\mathbf{C}}_1 : \bar{\boldsymbol{\varepsilon}}_1 + c_2 \mathbf{C}_2 : \bar{\boldsymbol{\varepsilon}}_2$, Eq. (4.11) for the averaged strain in the inclusions and for the averaged strain in the macroscopic volume $\bar{\boldsymbol{\varepsilon}} = c_1 \bar{\boldsymbol{\varepsilon}}_1 + c_2 \bar{\boldsymbol{\varepsilon}}_2$, the constitutive equation for the macro-volume (2.1) is written in the following form

$$\bar{\boldsymbol{\sigma}} = \mathbf{C}^* : \bar{\boldsymbol{\varepsilon}} - \frac{2c_1\tau_0}{9R_0 K_c} \left[\frac{1+\nu_c}{1-\nu_c} \right] \tilde{\mathbf{C}}_3 : \left(\overset{4}{\mathbf{I}} - \mathbf{L} : \tilde{\mathbf{C}}' \right)^{-1} : \overset{2}{\mathbf{I}} . \tag{4.13}$$

The relationship for the effective stiffness tensor are deduced to be

$$\mathbf{C}^* = c_1 \tilde{\mathbf{C}}_1 + c_2 \mathbf{C}_2 + c_1 \tilde{\mathbf{C}}_3 : \left(\overset{4}{\mathbf{I}} - \mathbf{L} : \tilde{\mathbf{C}}' \right)^{-1} : \left(c_2 \mathbf{L} : \tilde{\mathbf{C}}_3 \right), \tag{4.14}$$

with $\tilde{\mathbf{C}}_3 = \tilde{\mathbf{C}}_1 - \mathbf{C}_2$.

The relationship (4.13) between the macro stresses and the macro strains depends on the radius of the nanoparticles. The radius is also included in the expression for the effective stiffness tensor (4.14). The contribution of the surface residual stresses τ_0 is present in both terms on the right-hand side of Eq. (4.13). In the first term τ_0 appears via Eqs. (3.24) and (3.25), considering $\bar{\lambda}_s$ and $\bar{\mu}_s$ specified in the text following Eq. (3.20) while in the second term its presence is explicit. Its influence on the overall stiffness and on the average stresses in the material becomes increasingly pronounced as the size of the particles in the composite decreases. The last term in the right-hand side of Eq. (4.13) is the term defining the strain-independent average stresses in the composite, present exclusively due to surface tension τ_0 . In the present approach, the emergence of the second term in Eq. (4.13) is natural and the identification of the effective properties is unambiguous. The surface tension τ_0 is not considered in the investigations of Duan at al. (2005), Chen at al. (2007) and Brisard at al. (2010) with whose results the results obtained herein are compared. Finally, if the radius of a spherical particles R_0 is large, then $\hat{\lambda}_s$ and $\hat{\mu}_S \to 0$ and Eqs. (4.13), (4.14) reduce to the classical ones without the interface effect (Khoroshun et al. 1993; Nazarenko et al. 2009).

4.3 Scalar form of effective moduli

As shown in Appendix B Eq. (B.9), the following closed-form scalar expression for the effective bulk and shear moduli are extracted from a more general tensorial formula of Eq. (4.14)

$$K^* = c_1\left[K_1 + \hat{K}_S\right] + c_2 K_2 + \frac{9c_1c_2K\left[K_1 - K_2 + \hat{K}_S\right]^2}{1 - 9K\left[c_1K_2 + c_2\left(K_1 + \hat{K}_S\right) - K_c\right]}\ , \tag{4.15}$$

$$\mu^* = c_1\left[\mu_1 + \hat{\mu}_S\right] + c_2\mu_2 + \frac{4c_1c_2b\left[\mu_1 - \mu_2 + \hat{\mu}_S\right]^2}{1 - 4b\left[c_1\mu_2 + c_2\left(\mu_1 + \hat{\mu}_S\right) - \mu_c\right]}\ . \tag{4.16}$$

In this expression K_1, μ_1 and K_2, μ_2 are the bulk and shear moduli of the inclusions and of the matrix, respectively; K_c and μ_c are the bulk and shear moduli of the selected reference medium; K depends on *a* and *b* of Eq. (4.7) (as seen in Eq. (B.4a)) and, therefore, on the properties of the reference medium as well[3,4]. The resulting terms $\hat{K}_S = 4\left[\bar{\lambda}_S + \bar{\mu}_S\right]/\left[3R_0\right]$ and $\hat{\mu}_S = \left[7\mu_S + \lambda_S\right]/\left[5R_0\right]$ can be interpreted as an apparent increase in the bulk and shear moduli of the inhomogeneities associated with presence of the material surface surrounding them.

The additional variable $\hat{K}_S$ in the expression for the effective bulk moduli given in Eq. (4.15) is identical to the correction term obtained in a different way by Duan et al. (2005), Chen et al. (2007) and Brisard et al. (2010), who, in their solutions, used the same surface elasticity models (albeit without surface tension). In Brisard et al. (2010) only a lower bound on the bulk modulus was derived. Chen et al. (2007) presented quadratic equation (with coefficients to be determined using additional relations) for evaluation of μ^*. In Duan et al. (2005) some shear correction term is present but its form is very complicated and any direct comparisons are essentially impossible (other than through numerical values obtained for specific data). Its effects can be best seen in the impact it has on the overall properties of the composite, which is discussed in the next Section.

When $\hat{K}_S = 0$ and $\hat{\mu}_S = 0$ (no surface effects) and if it is recognized that $K = -\dfrac{1}{9\left[\lambda_c + 2\mu_c\right]}$, the following expressions for bulk and shear moduli are obtained from Eqs. (4.15), (4.16)

$$K_{cl}^* = \bar{K} + \frac{9c_1c_2\left[K_1 - K_2\right]^2}{-9\left[\lambda_c + 2\mu_c\right] - 9\left[c_1K_2 + c_2K_1 - K_c\right]} = \bar{K} - \frac{c_1c_2\left[K_1 - K_2\right]^2}{c_1K_2 + c_2K_1 + {}^4\!/_3\,\mu_c}\ , \tag{4.17}$$

$$\mu_{cl}^* = \bar{\mu} + \frac{4c_1c_2b\left[\mu_1 - \mu_2\right]^2}{1 - 4b\left[c_2\mu_1 + c_1\mu_2 - \mu_c\right]}\ . \tag{4.18}$$

As expected, expressions (4.17) as well as (4.18) are identical to the relationship obtained by the MCM without surface stresses (see in Khoroshun et al. 1993) for the bulk and shear moduli of the material with the same stochastic structure as the one considered here.

As remarked earlier, if the matrix is selected as the reference medium, Eq. (4.17) coincides with the upper Hashin-Shtrikman bound presented in Hashin and Shtrikman (1963). Brisard et al. (2010) extended the Hashin-Shtrikman bound formula to include surface elasticity. In their work, where a different approach is followed, the same parameter $\hat{K}_S$ emerges as a cor-

---

[3] If in the formula (4.15) for bulk modulus K_c and μ_c are taken to be equal to K_2 and μ_2 the results presented in the paper by Duan et al. (2005) are obtained.

[4] Formula (4.15) differs from the one presented by Nazarenko et al. (2014) by the way the surface effects were introduced in the two approaches. In Nazarenko et al. (2014) the surface effects are introduced as body forces accounted for via the surface integrals and, subsequently, averaged by the MCM. In the present contribution the surface effects are introduced via the notion of energy-equivalent inhomogeneity.

rection to the bulk modulus of the inclusions. This led to the lower Hashin-Shtrikman bound accounting for surface elasticity which are formally identical to those without surface effects but with the real bulk modulus of the inclusions replaced by their modified bulk modulus. In the present manuscript the parameters $\hat{K}_S$ and $\hat{\mu}_S$ also are appearing as a result of replacing the real inclusion with surface elasticity by a homogeneous one with effective properties (but without surface effects). The results of Duan et al. (2005), Chen et al. (2007) and Brisard et al. (2010) for bulk modulus can be obtained as a special case of the results presented in this paper if matrix is chosen as a reference medium. In Nazarenko et al. (2014) the value of $\hat{K}_S$ is the same as in all other papers mentioned here, but it enters the formula for the effective bulk modulus differently. So, the statistical averaging of the stochastic integral equation (3.1) is the reason why the equation for effective bulk modulus obtained in Nazarenko et al. (2014) cannot be obtained by replacing K_1 with $K_1 + \hat{K}_S$ in Eq. (4.17) which is valid for a material without the surface effects. This is also an indication that the mathematically rigorous way of introducing the surface effects as body forces presented in Nazarenko et al. (2014), and – for a different purpose – discussed at the beginning of this work, accounts for interaction between the constituents of the material in a different way than in the approaches proposed herein as well as in Brisard et al. (2010), Duan et al. (2005) and Chen et al. (2007), where substitution K_1 with $K_1 + \hat{K}_S$ was possible.

5. Numerical comparisons and discussion

5.1 Nanoporous aluminum

We consider an aluminum matrix with the properties $K_2 = 75.2\,\text{GPa}$ and $\nu_2 = 0.3$ containing spherical pores ($\mu_1 = K_1 = 0$). The free surface properties used in the present work are the same as those in Duan et al. (2005) and Miller and Shenoy (2000). In their articles two sets of surface properties are used, corresponding to the surfaces oriented along two different crystallographic directions: A for surface [100]: $\bar{\lambda}_S = \lambda_S + \tau_0 = 3.48912\ \text{N/m}$ and $\bar{\mu}_S = \mu_S - \tau_0 = -6.2178\ \text{N/m}$ and B for surface [111]: $\bar{\lambda}_S = \lambda_S + \tau_0 = 6.842\ \text{N/m}$ and $\bar{\mu}_S = \mu_S - \tau_0 = -0.3755\ \text{N/m}$.

The variation of the normalized bulk modulus K^*/K_{cl} with the void volume fractions calculated by the MCM in combination with equivalent inclusion approach – denoted by MCM EI – for the material containing spherical cavities of radius $R_0 = 5\,\text{nm}$, is shown in Fig. 1. The subscript “cl” is used to represent the results for the classical solution, i.e., the solution without interface stress. For comparison, the normalized bulk modulus for the same material obtained by the MCM in Nazarenko et al. (2014) (where the surface effects are represented by body forces) and on the basis of self-consistent scheme by Duan et al. (2005) are also shown in Fig.1. The bulk moduli shown in Fig.1 do not include the effects of surface tension.

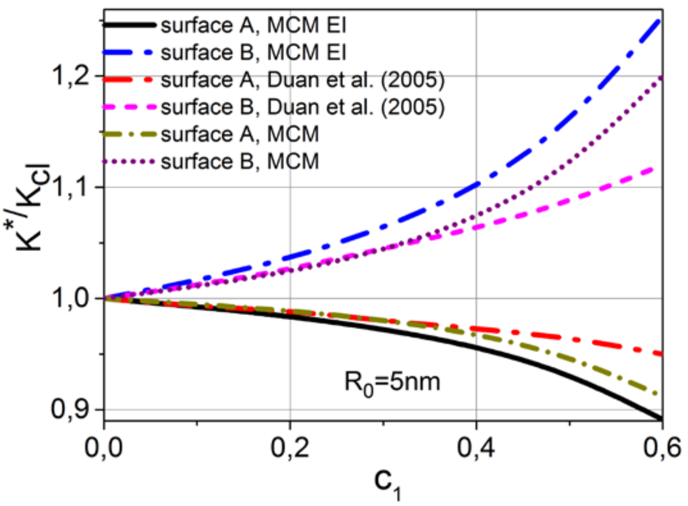

Fig.1: Dependence of the normalized bulk modulus K^{*}/K_{cl} on the void volume fraction c_1 for the radius of a spherical cavity $R_0 = 5$ (nm).

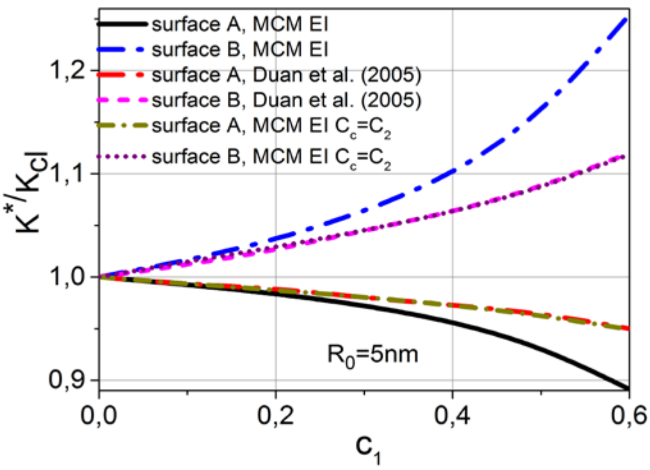

Fig.2: Dependence of the normalized bulk modulus K^{*}/K_{cl} on the void volume fraction c_1 for the radius of a spherical cavity $R_0 = 5$ (nm) and for $\mathbf{C}_c = \mathbf{C}_2$.

Fig.1 shows that the normalized bulk moduli obtained by different approaches are very similar for volume fraction of pores smaller than $c_1 = 0.3$. For higher volume fractions the values of those moduli differ by a larger amount, with both MCM and MCM EI approaches exhibiting larger influence of porosity than that of Duan et al. (2005). In addition to the results obtained using $\mathbf{C}_c$ advocated in this work, Fig.2 shows the normalized bulk moduli calculated by the equivalent inclusion approach and the MCM, but assuming that the reference medium is chosen as a matrix (i.e., using MCM EI with $\mathbf{C}_c = \mathbf{C}_2$). In this case, the bulk moduli obtained by the MCM approach are identical with the bulk moduli presented by Duan et al. (2005) for all values of pore volume fraction. It is interesting to note that Duan's results are obtained as a particular case of the presented approach, if it is assumed that $\mathbf{C}_c = \mathbf{C}_2$.

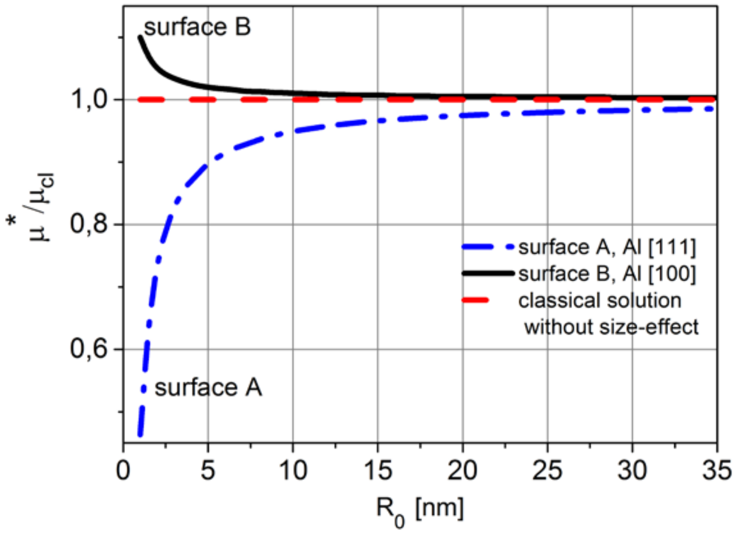

Fig.3: Dependence of the normalized shear modulus μ^* / μ_{cl} on the radius of a spherical cavity R_0(nm) for the void volume fraction $c_1 = 0.5$.

In Fig. 3 the normalized shear modulus μ^* / μ_{cl} for surface properties A and B is presented as a function of the cavity radius R_0 (nm), for the pore volume fraction fixed at c_1=0.5. The normalized shear modulus μ^* / μ_{cl} calculated for different void volume fractions for two different void radii is shown in Fig. 4. The surface effect on the effective bulk modulus becomes essentially negligible if the radius of the cavity is larger than 25 nm. As expected, this numerical illustration indicates that the surface effect is particularly significant for smaller sizes of pores. Comparison of Fig. 2 and Fig.5 leads to an interesting observation that contribution of surface effects in shear moduli is more significant than in bulk moduli for surface A and the opposite is true for surface B.

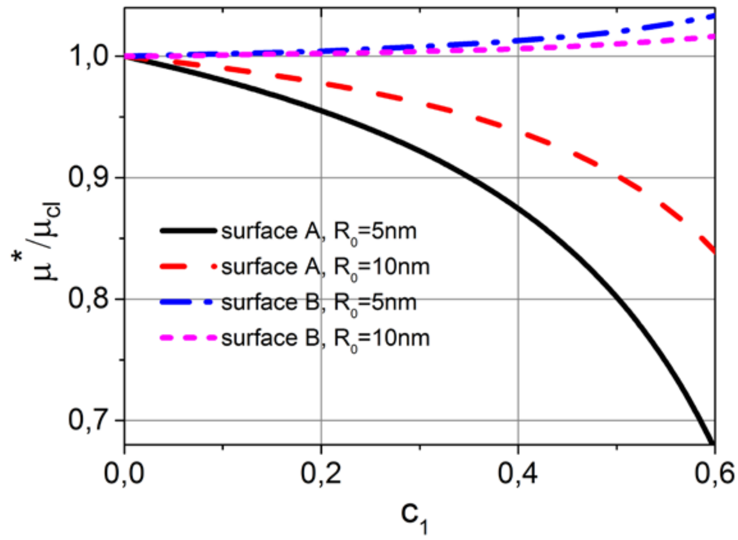

Fig.4: Dependences of the normalized bulk modulus μ^* / μ_{cl} on the void volume fraction c_1.

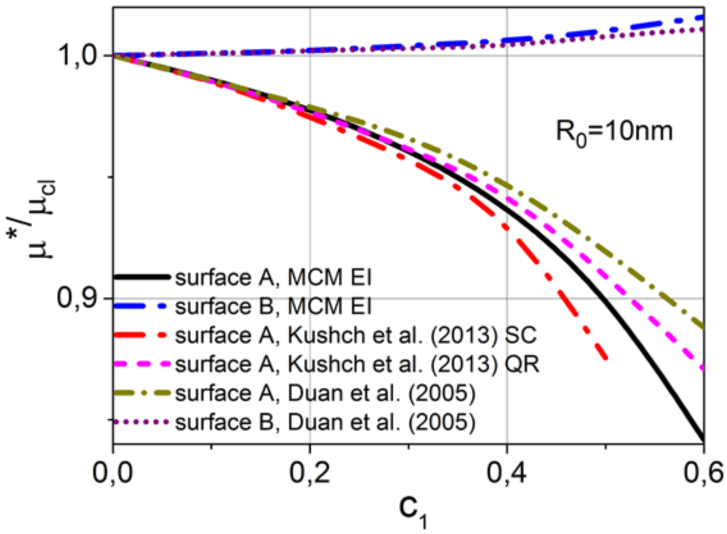

Fig.5: Dependences of the normalized shear modulus μ^* / μ_{cl} on the void volume fraction c_1 for the radius of a spherical cavity $R_0 = 10$ (nm). SC, QR: representative unit cell model with cubic structure (SC) and quasi-random (QR) array.

The variation of the normalized shear modulus μ^* / μ_{cl} with the void volume fractions calculated by the MCM in combination with equivalent inclusion approach MCM EI for the material containing spherical cavities of radius $R_0 = 10$ nm, is shown in Fig. 5. For comparison, the normalized shear moduli for the same material obtained on the basis of the self-consistent scheme by Duan et al. (2005) and on the basis of representative unit cell model, with both cubic structure and quasi-random array, by Kushch et al. (2013) are also shown in Fig.5. The normalized shear moduli obtained by different approaches are very similar for small volume fraction of pores, and for higher value of volume fraction the values of those moduli obtained in this paper are between the results for cubic structures and for quasi-random materials presented by Kushch et al. (2013). The good agreement of the present results with those of Kushch et al. (2013) exhibited in Fig. 5 provides an evidence that equivalent inclusion approach in combination with MCM can be used with sufficient high degree of precision for investigation of effective behavior of nano-materials.

The approach presented in this work is even more attractive in the analysis of more general cases. It can be extended for inclusions which have more complicated shapes as Eq. (A.13) for the stiffness tensor of the equivalent inclusion accounting for the presence of surface effects is valid for arbitrary shape of the inclusions. The MCM can also be applied to analyze materials containing inhomogeneities with more complex geometric and mechanical characteristics. Thus, the combination of the MCM approach and the notion of energy-equivalent inhomogeneity is quite powerful and its application to analyze more complicated materials is likely to be more interesting and more important. It is also likely to be more effective than other methods, given its capability to provide the closed-form results and its past success in analysis of composites with anisotropic components and spheroidal or ellipsoidal inclusions without surface effects see Khoroshun and Nazarenko (1990, 1992); Nazarenko et al. (2009).

Remark:

In this work K^* and μ^* were not computed separately of each other (considering hydrostatic loading separately from shear loading, as done by Duan et al. 2005; Chen et al. 2007; Kushch et al. 2013) but were extracted from the single tensorial formula for the composite's stiffness tensor obtained for arbitrary loading conditions, presented in Appendix B.

5.2 Nanoporous gold

As a second numerical example, nanoporous gold is considered. The Young's modulus of gold are given as $E_2 = 81\,\text{GPa}$ and $\nu_2 = 0.42$. The free surface properties of gold are extracted from the article of Shenoy (2005). The considered surface properties are taken as averaged of their values for different fcc crystal faces: $\lambda_S = -2.18875\ \text{N/m}$, $\mu_S = -2.5992\ \text{N/m}$ and $\tau_0 = 1.320865\ \text{N/m}$.

Nanoporous gold is an open cell porous material of random structure. At low densities, experimental results indicate that the macroscopically effective Young's modulus $\tilde{E}$ of cellular solids is related to the Young's modulus of their skeleton E_2 through the relation (Gibson and Ashby, 1988):

$$\frac{\tilde{E}}{E_2} = C\left[\frac{\tilde{\rho}}{\rho_2}\right]^n = C{c_2}^2, \tag{5.1}$$

where E_2 and ρ_2 are the Young's modulus and density of the solid skeleton, $\tilde{E}$ and $\tilde{\rho}$ are the effective Young's modulus and density of cellular solids and c_2 is volume fraction of solid. The constants C and n depend on the microstructure of the solid material. Experimental evidence suggests that $n = 2$ for open cells. For a ball-and-stick model presented in Huber et al. (2014) it is shown that C can be taken as

$$C = \frac{2}{\pi\sqrt{3}} \approx 0.37\ . \tag{5.2}$$

The Poisson's ratio has been found to be essentially independent of the volume fraction of solid (Gibson and Ashby, 1988). As the tensor of elastic constants of reference medium $\mathbf{C}_c$ should be close to the effective properties of the material, it is taken here to be in the form of Gibbs-Ashby estimation for open cell solids (Roberts and Garboczi, 2002; Huber et al. 2014):

$$E_c = \tilde{E} = C{c_2}^2 E_2\,,\ \nu_c = \nu_2\,, \tag{5.3}$$

where E_2, E_c and ν_2, ν_c are Young's modulus and Poisson's ratio of gold and reference medium, respectively.

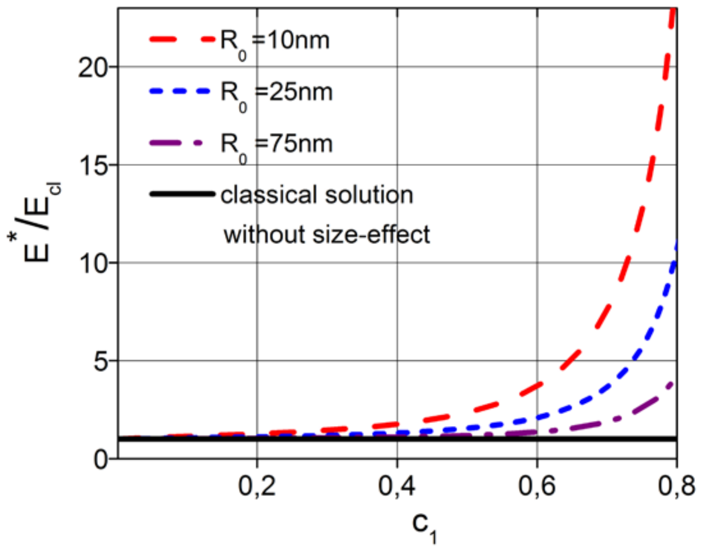

Fig.6: Nanoporous gold: Dependence of the normalized Young's modulus E^* / E_{cl} on the void volume fraction c_1.

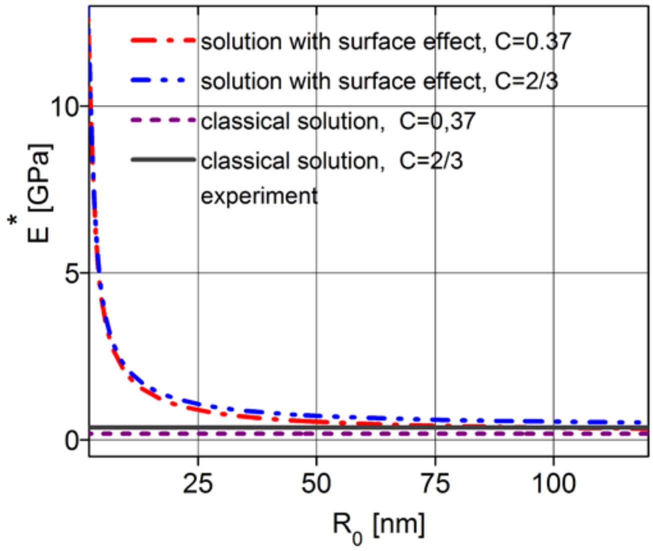

Fig.7: Dependence of the effective Young's modulus E^* on the radius of a ligament R_0(nm) for the void volume fraction $c_1 = 0.73$.

In the present case, the mean curvature of the pores κ is defined by the mean curvature of ligaments[5]. The ligaments have ellipsoidal shape and are randomly distributed and oriented. The effective properties for such a structure are close to the structure with quasi-spherical ligaments. The mean curvature of the pores in this case can be taken as $\kappa = 1/R_0$, where R_0 is the mean ligament radius.

The normalized Young's moduli vs. the void volume fraction for various ligament radii with $C = 0.37$ are shown in Fig. 6. As in the case of nano-porous aluminum, the surface effect on Young's modulus becomes significant for smaller sizes of ligaments and increases with decreasing ligament size, in agreement with the experimental investigations (Huber et al. 2014; Wang and Weissmüller 2013 among other).

The effective Young's moduli vs. ligament radius for the void volume fraction $c_1 = 0.74$ with and without accounting for surface effects for different values of parameter C are presented in Fig. 7. Qualitatively, the tendency observed in experimental investigations (increasing Young's modulus with decreasing ligament radius) is well captured.

6. Conclusions

A new mathematical model for investigation of the effective properties of a material with randomly distributed nanoparticles, which requires a special treatment of the surface between matrix and nanoparticles, has been proposed. The surface effects are introduced via Gurtin-Murdoch equations (Gurtin and Murdoch, 1975, 1978) describing properties of the ma-

[5] As opposed to nanoporous Al (where $\kappa = -1/R_0$), in the case of nanoporous gold the mean curvature of the cavities is equal to the mean curvature of ligaments taken with the plus sign. The sign is to be changed because, in contrast with the case of Al, the vector **n** normal to the interface, and directed away from the cavities, points towards the interface's center of curvature (which coincides with the center of ligament).

trix/nanoparticles interface, which are added to the system of stochastic differential equations formulated within the framework of linear elasticity. However, these surface effects are accounted for in a different way than in the past papers.

While the general ingredients of the approach are the same as in the previous work of these authors, Nazarenko et al. (2014), the way the surface effects are accounted for is here entirely different. The notion of energy-equivalent inhomogeneities was introduced in this work for the first time to this end and combined with the MCM. This not only allowed to reproduce the result for the effective bulk modulus obtained in Nazarenko et al. (2014) but enabled evaluation of the effective shear modulus as well. There are two critical elements of the proposed approach. The first one is the right selection of the reference medium (in the MCM) which, as argued in Section 3, should be made independently of the notion of equivalent inhomogeneity. The second element is that the energy-equivalent inhomogeneity is determined assuming their uniform state of strains. Apart from the fact that the equivalent properties (including the effective properties of the composites) are always determined assuming globally homogeneous deformation pattern, this assumption is particularly suitable in the context of the MCM version used here. As mentioned in the main body of the work, the restriction of the MCM to the two-point conditional moments adopted here is effectively tantamount to the assumption that deformation of the inhomogeneities is uniform. This is in perfect agreement with the way the effective inhomogeneity is defined in Section 3. Incidentally, the strain fluctuations in the inclusions are also assumed to vanish in all deterministic methods based on the Eshelby's solution.

As a numerical illustration of the presented approach, two nanoporous materials are studied – nanoporous aluminum and nanoporous gold. The bulk and shear moduli of aluminum has been analyzed for varying volume content and varying radius of the nano-cavities. Young moduls of the nanoporous gold was investigated in terms of its dependence on the gold volume fractions and on the radius of the gold ligaments.

The size effect introduced due to addition of the residual stresses and elasticity on the matrix/nanoparticles interface in nanoporous aluminum (surface of nano-pores in the chosen numerical examples) is accounted for in the expressions for effective bulk and shear moduli of the composite. It has been shown that the proposed approach is capable to reveal that the surface effect is significant for smaller sizes of pores. It is also able to capture the qualitative influence that a particular type of the material surface between matrix and nanoparticles has on the effective properties of porous aluminum with random distribution of pores. Comparison with results obtained on the basis of the self-consistent scheme and representative unit cell method shows that proposed approach is comparable in accuracy and is successfully used for investigation of particulate nano-materials.

The general effectiveness of the MCM approach, documented in several other publications (Khoroshun and Nazarenko 1990, 1992; Nazarenko et al. 2009), combined with its congruity with the special definition of the equivalent inhomogeneity has likely been the reason that led to the results which are so close to those obtained by other, quite involving approaches. It is particularly remarkable that the closed-form formulas provided in this work are in such a good agreement with the results of Kushch et al. (2013), which are based on the precise solution of the differential equations of the problem and on different extraction of the effective constants from those solutions.

The Young's moduli of nanoporous gold have been analyzed for varying volume content of the nano-cavities, varying radius of the ligaments and for two different values of the stiffness tensor of the reference medium. This analysis has shown qualitatively the same tendency as that seen in experimental observations of this material (increasing Young's modulus with decreasing ligament radius) and has indicated a possibility for further development of the presented model and its application to new nano-materials.

To conclude it is worth mentioning that the definition of the energy-equivalent inhomogeneity is general and can be used in the case of inhomogeneities of other shapes than spherical, e.g., ellipsoidal or cylindrical. The conceptual features of the approach would remain the same. Whether or not the results obtained would be of the same quality is an open issue, which needs to be investigated. Such investigation is greatly facilitated by combining the notion of the energy-equivalent inhomogeneity with the MCM. Both can be applied for analysis of materials containing inhomogeneities with more complex geometric and mechanical characteristics, and their important characteristic is ability to provide closed-form expressions for the effective properties of nano-composites. Closed-form results have an important intellectual value and are always the best if the influence of different problem parameters needs to be inferred either quantitatively or qualitatively.

Appendix A. Formulas for the properties of equivalent inclusion.

A1. Energy equivalence and modification of the bulk properties of the inclusions.

Although most of this work is related to spherical inhomogeneities, the development presented in this Appendix is general to underscore the fact that, with some additional technical effort, the approach is applicable to more general shapes.

Let's assume that the surface of an inhomogeneity is locally parameterized by ξ^{Λ}, $\Lambda \in \{1,2\}$, that is the position vector of a point on that surface is expressed as $\mathbf{r}(\xi^{\Lambda})$. Then, one can define vectors $\mathbf{G}_{\Lambda}$

$$\mathbf{G}_{\Lambda} = \frac{\partial \mathbf{r}}{\partial \xi^{\Lambda}} \equiv \mathbf{r},_{\Lambda} \quad , \tag{A.1}$$

which form~~s~~ the vector basis in the linear space tangent to the surface *S*, and called the natural basis. Another basis in the same tangent space, denoted by $\mathbf{G}^{\Delta}$ and called dual or reciprocal, is defined via the following orthogonality condition

$$\mathbf{G}_{\Lambda} \cdot \mathbf{G}^{\Delta} = \delta^{\Delta}{}_{\Lambda} \, , \tag{A.2}$$

where the symbol "•" represents the inner product of vectors and $\delta^{\Delta}{}_{\Lambda}$ is the Kronecker delta.

Assuming that the inhomogeneity deforms uniformly, and the materials of both the inhomogeneity and its surface are linearly elastic, their combined strain energy is defined in Eq. (3.18) with

$$\bar{\boldsymbol{\varepsilon}}_1 : \mathbf{C}_1 : \bar{\boldsymbol{\varepsilon}}_1 = 2\mu_1 \bar{\boldsymbol{\varepsilon}}_1 : \bar{\boldsymbol{\varepsilon}}_1 + \lambda_1 \mathrm{tr}(\bar{\boldsymbol{\varepsilon}}_1)^2 \tag{A.3a}$$

$$\boldsymbol{\varepsilon}_S : \mathbf{C}_S : \boldsymbol{\varepsilon}_S = 2\overline{\mu}_S \boldsymbol{\varepsilon}_S : \boldsymbol{\varepsilon}_S + \overline{\lambda}_S \mathrm{tr}(\boldsymbol{\varepsilon}_S)^2 \tag{A.3b}$$

In addition, since the matrix/inhomogeneities interfaces are assumed to be coherent, the surface strains present in that equation are related to the strains within the volume of the inhomogeneity. Thus, in order to express the energy defined in Eq. (3.18) as a function of the constant strain $\bar{\varepsilon}_1$ in the volume of the inhomogeneity, the surface strains ε_S need to be evaluated in terms of $\bar{\varepsilon}_1$ at every point of the surface.

To this end it is first noted that one possible representation of the surface strains is:

$$\boldsymbol{\varepsilon}_S = \varepsilon_{\Delta\Lambda} \mathbf{G}^{\Delta} \otimes \mathbf{G}^{\Lambda} \, , \ \Delta, \Lambda \in \{1,2\}, \tag{A.4}$$

It is also noted that, at each point of the surface, the strain tensor within the volume of the inhomogeneity may be represented as follows:

$$\bar{\boldsymbol{\varepsilon}}_1 = \varepsilon_{\Delta\Lambda}\mathbf{G}^{\Delta} \otimes \mathbf{G}^{\Lambda} + \varepsilon_{\Delta 3}\mathbf{G}^{\Delta} \otimes \mathbf{n} + \varepsilon_{3\Lambda}\mathbf{n} \otimes \mathbf{G}^{\Lambda} + \varepsilon_{33}\mathbf{n} \otimes \mathbf{n} = \varepsilon_{ij}\mathbf{e}^i \otimes \mathbf{e}^j \qquad \Delta, \Lambda \in \{1, 2\} \tag{A.5}$$

which, in view of Eq. (A2) and the properties $\mathbf{n} \cdot \mathbf{G}^{\Delta} = \mathbf{n} \cdot \mathbf{G}_{\Delta} = 0$, implies that

$$\varepsilon_{\Delta\Lambda} = \bar{\boldsymbol{\varepsilon}}_1 : (\mathbf{G}_{\Delta} \otimes \mathbf{G}_{\Lambda}) \tag{A.6}$$

Consequently, the surface strain tensor of Eq. (A.4) may be related to $\bar{\boldsymbol{\varepsilon}}_1$ by the following formula

$$\boldsymbol{\varepsilon}_S = \bar{\boldsymbol{\varepsilon}}_1 : \overset{4}{\mathbf{I}}_S \tag{A.7}$$

where

$$\overset{4}{\mathbf{I}}_S = \mathbf{G}_{\Delta} \otimes \mathbf{G}_{\Lambda} \otimes \mathbf{G}^{\Delta} \otimes \mathbf{G}^{\Lambda}, \quad \Delta, \Lambda \in \{1, 2\}. \tag{A.8}$$

With the above result, and with the analogical result in the volume of the inhomogeneity, the following formulas are obtained

$$2\mu_1 \bar{\boldsymbol{\varepsilon}}_1 : \bar{\boldsymbol{\varepsilon}}_1 = \bar{\boldsymbol{\varepsilon}}_1 : \left(2\mu_1 \overset{4}{\mathbf{I}}\right) : \bar{\boldsymbol{\varepsilon}}_1, \tag{A.9a}$$

$$2\bar{\mu}_S \boldsymbol{\varepsilon}_S : \boldsymbol{\varepsilon}_S = \bar{\boldsymbol{\varepsilon}}_1 : \left(2\bar{\mu}_S \overset{4}{\mathbf{I}}_S\right) : \bar{\boldsymbol{\varepsilon}}_1 . \tag{A.9b}$$

Likewise, considering that

$$\operatorname{tr} \boldsymbol{\varepsilon}_S = \boldsymbol{\varepsilon}_S : \overset{2}{\mathbf{I}}_S = \boldsymbol{\varepsilon}_1 : \overset{2}{\mathbf{I}}_S \quad \text{and} \quad \operatorname{tr} \bar{\boldsymbol{\varepsilon}}_1 = \vec{\boldsymbol{\varepsilon}}_1 : \overset{2}{\mathbf{I}} \tag{A.10}$$

one obtains

$$\lambda_1 \operatorname{tr}(\bar{\boldsymbol{\varepsilon}}_1)^2 = \bar{\boldsymbol{\varepsilon}}_1 : \left(\lambda_1 \overset{2}{\mathbf{I}} \otimes \overset{2}{\mathbf{I}}\right) : \bar{\boldsymbol{\varepsilon}}_1, \tag{A.11a}$$

$$\bar{\lambda}_S \operatorname{tr}(\boldsymbol{\varepsilon}_S)^2 = \bar{\boldsymbol{\varepsilon}}_1 : \left(\bar{\lambda}_S \overset{2}{\mathbf{I}}_S \otimes \overset{2}{\mathbf{I}}_S\right) : \bar{\boldsymbol{\varepsilon}}_1, \tag{A.11b}$$

with

$$\overset{2}{\mathbf{I}}_S \otimes \overset{2}{\mathbf{I}}_S = \mathbf{G}_{\Delta} \otimes \mathbf{G}^{\Delta} \otimes \mathbf{G}_{\Lambda} \otimes \mathbf{G}^{\Lambda} \quad \Delta, \Lambda \in \{1, 2\}. \tag{A.12}$$

Introducing Eqs. (A.9a,b) and (A.11a,b) into Eqs. (A.3a,b), observing Eqs. (3.18) and (3.21) and taking into account that $\bar{\varepsilon}_1$ are constant and arbitrary one obtains:

$$\bar{\mathbf{C}}_1 = \mathbf{C}_1 + \frac{1}{2V_I} \oint_{S_I} \left(2\bar{\mu}_S \overset{4}{\mathbf{I}}_S + \bar{\lambda}_S \overset{2}{\mathbf{I}}_S \otimes \overset{2}{\mathbf{I}}_S\right) d\, S_I . \tag{A.13}$$

In the main body of the paper spherical inhomogeneities are considered and tensors $\overset{4}{\mathbf{I}}_S$ as well as $\overset{2}{\mathbf{I}}_S \otimes \overset{2}{\mathbf{I}}_S$ are function of the spherical coordinates φ and θ

A2. Representation of tensors $\overset{4}{\mathbf{I}}_S$ and $\overset{2}{\mathbf{I}}_S \otimes \overset{2}{\mathbf{I}}_S$ in Cartesian coordinate system

Eq. (A.13) is valid for arbitrary shape of inhomogeneities. In this contribution only spherical inhomogeneities are considered. In order to determine the properties of equivalent inhomogeneities the expressions for Cartesian components of tensors $\overset{4}{\mathbf{I}}_S$ as well as $\overset{2}{\mathbf{I}}_S \otimes \overset{2}{\mathbf{I}}_S$ are needed in the surface integral of Eq. (A.13).

In the Cartesian coordinate system *x-y-z*, the position vector $\mathbf{r}$ of a point on the sphere may be expressed as follows:

$$\mathbf{r} = \rho\begin{bmatrix} \cos\varphi\sin\theta \\ \sin\varphi\sin\theta \\ -\cos\theta \end{bmatrix}, \quad 0\leq\varphi\leq 2\pi, \quad 0\leq\theta\leq\pi. \qquad \text{(A.14)}$$

Consequently, the local vectors of the natural basis $\mathbf{G}_\Delta$ are

$$\mathbf{G}_1 = R,_1 = \rho\begin{bmatrix} -\sin\varphi\sin\theta \\ \cos\varphi\sin\theta \\ 0 \end{bmatrix}, \quad \mathbf{G}_2 = R,_2 = \rho\begin{bmatrix} \cos\varphi\cos\theta \\ \sin\varphi\cos\theta \\ \sin\theta \end{bmatrix}, \quad \mathbf{G}_3 = \frac{R}{\rho} = n = \begin{bmatrix} \cos s\,\varphi\sin\theta \\ \sin\varphi\sin\theta \\ -\cos\theta \end{bmatrix}. \qquad \text{(A.15)}$$

and the magnitudes of those vectors are:

$$|\mathbf{G}_1| = \rho\sin\theta, \quad |\mathbf{G}_2| = \rho, \quad n = 1. \qquad \text{(A.16)}$$

The vectors of the dual (or reciprocal) basis are defined via:

$$\mathbf{G}_\Delta \cdot \mathbf{G}^\Lambda = \delta_\Delta^\Lambda, \qquad \text{(A.17)}$$

are found to be

$$\mathbf{G}^1 = \frac{1}{\rho}\begin{bmatrix} -\sin\varphi/\sin\theta \\ \cos\varphi/\sin\theta \\ 0 \end{bmatrix}, \quad \mathbf{G}^2 = \frac{1}{\rho}\begin{bmatrix} \cos\varphi\cos\theta \\ \sin\varphi\cos\theta \\ \sin\theta \end{bmatrix}, \quad \mathbf{G}_3 = \mathbf{G}^3 = n = \begin{bmatrix} \cos\varphi\sin\theta \\ \sin\varphi\sin\theta \\ -\cos\theta \end{bmatrix}. \qquad \text{(A.18)}$$

The magnitudes of those vectors are

$$|\mathbf{G}^1| = 1/(\rho\sin\theta) \quad |\mathbf{G}^2| = 1/\rho \quad |\mathbf{G}^3| = n = 1 \qquad \text{(A.19)}$$

Given that $\mathbf{G}_K$ are parallel to $\mathbf{G}^K$ for $K \in \{1, 2, 3\}$, the unit vectors, parallel to $\mathbf{G}_K$ and $\mathbf{G}^K$ are:

$$\overline{\mathbf{G}}_1 = \frac{\mathbf{G}_1}{|\mathbf{G}_1|} = \begin{bmatrix} -\sin\varphi \\ \cos\varphi \\ 0 \end{bmatrix}, \quad \overline{\mathbf{G}}_2 = \frac{\mathbf{G}_2}{|\mathbf{G}_2|} = \begin{bmatrix} \cos\varphi\cos\theta \\ \sin\varphi\cos\theta \\ \sin\theta \end{bmatrix}, \quad \overline{\mathbf{G}}_3 = n = \begin{bmatrix} \cos\varphi\sin\theta \\ \sin\varphi\sin\theta \\ -\cos\theta \end{bmatrix}. \qquad \text{(A.20)}$$

Thus accounting for Eqs (A.9) and (A.12) one obtains:

$$\overset{4}{\mathbf{I}}_S = \sum_{\Delta=1}^{2}\sum_{\Lambda=1}^{2} \underbrace{|\mathbf{G}_\Delta||\mathbf{G}^\Delta|}_{=1}\underbrace{|\mathbf{G}_\Lambda||\mathbf{G}^\Lambda|}_{=1} \overline{\mathbf{G}}_\Delta \otimes \overline{\mathbf{G}}_\Lambda \otimes \overline{\mathbf{G}}^\Delta \otimes \overline{\mathbf{G}}^\Lambda, \qquad \text{(A.21)}$$

which leads to the following formulas for the surface tenors involved in Eq. (A.13)

$$\overset{4}{\mathbf{I}}_S = \overline{\mathbf{G}}_1 \otimes \overline{\mathbf{G}}_1 \otimes \overline{\mathbf{G}}_1 \otimes \overline{\mathbf{G}}_1 + \overline{\mathbf{G}}_1 \otimes \overline{\mathbf{G}}_2 \otimes \overline{\mathbf{G}}_1 \otimes \overline{\mathbf{G}}_2 + \overline{\mathbf{G}}_2 \otimes \overline{\mathbf{G}}_1 \otimes \overline{\mathbf{G}}_2 \otimes \overline{\mathbf{G}}_1 + \overline{\mathbf{G}}_2 \otimes \overline{\mathbf{G}}_2 \otimes \overline{\mathbf{G}}_2 \otimes \overline{\mathbf{G}}_2, \qquad \text{(A.21a)}$$

$$\overset{2}{\mathbf{I}}_S \otimes \overset{2}{\mathbf{I}}_S = \overline{\mathbf{G}}_1 \otimes \overline{\mathbf{G}}_1 \otimes \overline{\mathbf{G}}_1 \otimes \overline{\mathbf{G}}_1 + \overline{\mathbf{G}}_1 \otimes \overline{\mathbf{G}}_1 \otimes \overline{\mathbf{G}}_2 \otimes \overline{\mathbf{G}}_2 + \overline{\mathbf{G}}_2 \otimes \overline{\mathbf{G}}_2 \otimes \overline{\mathbf{G}}_1 \otimes \overline{\mathbf{G}}_1 + \overline{\mathbf{G}}_2 \otimes \overline{\mathbf{G}}_2 \otimes \overline{\mathbf{G}}_2 \otimes \overline{\mathbf{G}}_2. \qquad \text{(A.21b)}$$

The Cartesian components of those tensors are obtained if Eqs. (A.20) are inserted into Eqs. (A.21a) and (A.21b).

A3. Evaluation of $\hat{\lambda}_S$ and $\hat{\mu}_S$

Evaluation of the integral part of Eq. (A.13) is straightforward, however the results of the integration are listed here for completeness and illustration.

The following integral well represents the level of difficulty involved:

$$\frac{3}{4\pi R_0^3}\int_0^{\pi}\int_0^{2\pi}\overset{4}{I}_{S(1111)}\,R_0^2\sin\theta\,\mathrm{d}\varphi\,\mathrm{d}\theta=\frac{3}{4\pi R_0}\int_0^{\pi}\int_0^{2\pi}\left(\sin^4\varphi+2\cos^2\varphi\sin^2\varphi\cos^2\theta+\cos^4\varphi\cos^4\theta\right)\sin\theta\,\mathrm{d}\varphi\,\mathrm{d}\theta=\frac{8}{5R_0},$$

If the remaining integrals are evaluated the following results are obtained:

$$\frac{3}{4\pi R_0^3}\int_0^{\pi}\int_0^{2\pi}\overset{4}{I}_{S(1122)}\,R_0^2\sin\theta\,\mathrm{d}\varphi\,\mathrm{d}\theta=\frac{1}{5R_0},\qquad \frac{3}{4\pi R_0^3}\int_0^{\pi}\int_0^{2\pi}\overset{4}{I}_{S(1212)}\,R_0^2\sin\theta\,\mathrm{d}\varphi\,\mathrm{d}\theta=\frac{6}{5R_0},$$

$$\frac{3}{4\pi R_0^3}\int_0^{\pi}\int_0^{2\pi}\overset{4}{I}_{S(2112)}\,R_0^2\sin\theta\,\mathrm{d}\varphi\,\mathrm{d}\theta=\frac{1}{5R_0},\qquad \frac{3}{4\pi R_0^3}\int_0^{\pi}\int_0^{2\pi}\overset{2}{I}_S\otimes\overset{2}{I}_{S(1111)}\,R_0^2\sin\theta\,\mathrm{d}\varphi\,\mathrm{d}\theta=\frac{8}{5R_0},$$

$$\frac{3}{4\pi R_0^3}\int_0^{\pi}\int_0^{2\pi}\overset{2}{I}_S\otimes\overset{2}{I}_{S(1122)}\,R_0^2\sin\theta\,\mathrm{d}\varphi\,\mathrm{d}\theta=\frac{6}{5R_0},\qquad \frac{3}{4\pi R_0^3}\int_0^{\pi}\int_0^{2\pi}\overset{2}{I}_S\otimes\overset{2}{I}_{S(1212)}\,R_0^2\sin\theta\,\mathrm{d}\varphi\,\mathrm{d}\theta=\frac{1}{5R_0},$$

$$\frac{3}{4\pi R_0^3}\int_0^{\pi}\int_0^{2\pi}\overset{2}{I}_S\otimes\overset{2}{I}_{S(2112)}\,R_0^2\sin\theta\,\mathrm{d}\varphi\,\mathrm{d}\theta=\frac{1}{5R_0},$$

with zero values in all of the remaining cases. Consequently, the following non-vanishing components of tensor $\hat{C}_{ijkl}$ from Eq. (3.23b) result

$$\hat{C}_{1111}=\frac{3}{4\pi R_0}\int_0^{2\pi}\int_0^{\pi}\left(2\overline{\mu}_S\overset{4}{I}_{S(1111)}+\overline{\lambda}_S\overset{2}{I}_S\otimes\overset{2}{I}_{S(1111)}\right)\sin\theta\,d\varphi\,d\theta=\frac{8}{5R_0}\left[2\overline{\mu}_S+\overline{\lambda}_S\right], \tag{A.23a}$$

$$\hat{C}_{1122}=\hat{C}_{1133}=\frac{3}{4\pi R_0}\int_0^{2\pi}\int_0^{\pi}\left(2\overline{\mu}_S\overset{4}{I}_{S(1122)}+\overline{\lambda}_S\overset{2}{I}_S\otimes\overset{2}{I}_{S(1122)}\right)\sin\theta\,d\varphi\,d\theta=\frac{2}{5R_0}\left[\overline{\mu}_S+3\overline{\lambda}_S\right], \tag{A.23b}$$

$$\hat{C}_{1212}=\hat{C}_{2121}=\frac{3}{4\pi R_0}\int_0^{2\pi}\int_0^{\pi}\left(2\overline{\mu}_S\overset{4}{I}_{S(1212)}+\overline{\lambda}_S\overset{2}{I}_S\otimes\overset{2}{I}_{S(1212)}\right)\sin\theta\,d\varphi\,d\theta=\frac{1}{5R_0}\left[12\overline{\mu}_S+\overline{\lambda}_S\right], \tag{A.23c}$$

$$\hat{C}_{2112}=\hat{C}_{1221}=\frac{3}{4\pi R_0}\int_0^{2\pi}\int_0^{\pi}\left(2\overline{\mu}_S\overset{4}{I}_{S(2112)}+\overline{\lambda}_S\overset{2}{I}_S\otimes\overset{2}{I}_{S(2112)}\right)\sin\theta\,d\varphi\,d\theta=\frac{1}{5R_0}\left[2\overline{\mu}_S+\overline{\lambda}_S\right], \tag{A.23d}$$

As expected, because of the spherical geometry of the inhomogeneities, the above components characterize an isotropic tensor which can be characterized by common Lame's parameters as follows

$$\hat{\mathrm{K}}_S=\frac{1}{3}\left[\hat{C}_{1111}+\hat{C}_{1122}+\hat{C}_{1133}\right]=\frac{4}{3R_0}\left[\overline{\mu}_S+\overline{\lambda}_S\right], \tag{A.24a}$$

$$\hat{\lambda}_S=\hat{C}_{1122}=\frac{2}{5R_0}\left[\overline{\mu}_S+3\overline{\lambda}_S\right], \tag{A.24b}$$

$$2\hat{\mu}_S=\hat{C}_{1111}-\hat{C}_{1122}=\hat{C}_{1212}+\hat{C}_{2112}=\frac{2}{5R_0}\left[7\overline{\mu}_S+\overline{\lambda}_S\right]. \tag{A.24c}$$

Appendix B. Scalar formulas for the effective material properties.

The operations presented here are standard, but they are reproduced here after Nazarenko et al. (2014) for the present paper to be self-contained.

All three-dimensional isotropic stiffness tensors of Eqs. (3.19), (3.24) may be cast in the following equivalent forms (as a sum of the volumetric and deviatoric parts):

$$\mathbf{C}_1 = [3\lambda_1 + 2\mu_1]\left[\frac{1}{3}\overset{2}{\mathbf{I}}\otimes\overset{2}{\mathbf{I}}\right] + 2\mu_1\left[\overset{4}{\mathbf{I}} - \frac{1}{3}\overset{2}{\mathbf{I}}\otimes\overset{2}{\mathbf{I}}\right] = 3K_1\mathbf{H} + 2\mu_1\mathbf{D},$$

$$\mathbf{C}_2 = [3\lambda_2 + 2\mu_2]\left[\frac{1}{3}\overset{2}{\mathbf{I}}\otimes\overset{2}{\mathbf{I}}\right] + 2\mu_2\left[\overset{4}{\mathbf{I}} - \frac{1}{3}\overset{2}{\mathbf{I}}\otimes\overset{2}{\mathbf{I}}\right] = 3K_2\mathbf{H} + 2\mu_2\mathbf{D},$$

$$\tilde{\mathbf{C}}_1 == \left[3\left(\lambda_1 + \hat{\lambda}_S\right) + 2\left(\mu_1 + \hat{\mu}_S\right)\right]\left[\frac{1}{3}\overset{2}{\mathbf{I}}\otimes\overset{2}{\mathbf{I}}\right] + 2\left(\mu_1 + \hat{\mu}_S\right)\left[\overset{4}{\mathbf{I}} - \frac{1}{3}\overset{2}{\mathbf{I}}\otimes\overset{2}{\mathbf{I}}\right] = 3\left(K_1 + \hat{K}_S\right)\mathbf{H} + 2\left(\mu_1 + \hat{\mu}_S\right)\mathbf{D}, \quad \text{(B.1)}$$

where $\lambda_1, \mu_1, \lambda_2, \mu_2$ are Lamé constants characterizing the bulk material of the nano-inhomogeneities and the material of the matrix, respectively, $K_1 = [3\lambda_1 + 2\mu_1]/3$, $K_2 = [3\lambda_2 + 2\mu_2]/3$ are the bulk moduli of the corresponding materials, $\hat{\lambda}_S$, $\hat{\mu}_S$, and $\hat{K}_S = \left[3\hat{\lambda}_S + 2\hat{\mu}_S\right]/3$ are the contributions of surface elasticity defined in Appendix A, Eq.(A.24a-c), which depend on the radius of inclusion R_0; the rank four tensors $\mathbf{H} = \frac{1}{3}\overset{2}{\mathbf{I}}\otimes\overset{2}{\mathbf{I}}$ and $\mathbf{D} = \overset{4}{\mathbf{I}} - \frac{1}{3}\overset{2}{\mathbf{I}}\otimes\overset{2}{\mathbf{I}}$ are the volumetric (or hydrostatic) and deviatoric fourth-order projectors, correspondingly (see details in Nazarenko et al. 2014).

All fourth-order tensors present in Eq. (4.14) are isotropic and have the form expressed in the right-hand side of Eq. (B.1). For the superposition of the operations those tensors represent (i.e., their multiplication, or double contraction) one has

$$\mathbf{C}_1 : \mathbf{C}_2 = \mathbf{C}_2 : \mathbf{C}_1 = 9K_1K_2\mathbf{H} + 4\mu_1\mu_2\mathbf{D}, \quad \text{(B.2)}$$

and for the inversion (illustrated only for tensor $\mathbf{C}_1$)

$$\mathbf{C}_1^{-1} = \frac{1}{3K_1}\mathbf{H} + \frac{1}{2\mu_1}\mathbf{D}. \quad \text{(B.3)}$$

Observing Eqs. (B.1)-(B.3) the tensors involved in Eq. (4.14) and defined in the main body of the paper can be presented in the following forms:

$$\mathbf{L} = [3a + 2b]\left(\frac{1}{3}\overset{2}{\mathbf{I}}\otimes\overset{2}{\mathbf{I}}\right) + 2b\left(\overset{4}{\mathbf{I}} - \frac{1}{3}\overset{2}{\mathbf{I}}\otimes\overset{2}{\mathbf{I}}\right) = 3K\mathbf{H} + 2b\mathbf{D}, \quad \text{(B.4a)}$$

$$\tilde{\mathbf{C}}_3 = 3\left[K_1 + \hat{K}_S - K_2\right]\mathbf{H} + 2\left[\mu_1 + \hat{\mu}_S - \mu_2\right]\mathbf{D} = 3\tilde{K}_3\mathbf{H} + 2\tilde{\mu}_3\mathbf{D}, \quad \text{(B.4b)}$$

$$\tilde{\mathbf{C}}_4 = 3\left[c_2\left(K_1 + \hat{K}_S\right) + c_1K_2\right]\mathbf{H} + 2\left[c_2\left(\mu_1 + \hat{\mu}_S\right) + c_1\mu_2\right]\mathbf{D} = 3\tilde{K}_4\mathbf{H} + 2\tilde{\mu}_4\mathbf{D}, \quad \text{(B.4c)}$$

$$\overline{\mathbf{C}} = 3[c_1K_1 + c_2K_2]\mathbf{H} + 2[c_1\mu_1 + c_2\mu_2]\mathbf{D} = 3\overline{K}\mathbf{H} + 2\overline{\mu}\,\mathbf{D}, \quad \text{(B.4d)}$$

$$\overline{\overline{\mathbf{C}}} = 3\left[\frac{K_1K_2}{c_1K_2 + c_2K_1}\right]\mathbf{H} + 2\left[\frac{\mu_1\mu_2}{c_1\mu_2 + c_2\mu_1}\right]\mathbf{D} = 3\overline{\overline{K}}\mathbf{H} + 2\overline{\overline{\mu}}\mathbf{D}. \quad \text{(B.4e)}$$

$$\mathbf{C}_c = 3K_c\mathbf{H} + 2\mu_c\mathbf{D}, \quad \mathbf{C}_c = \overline{\mathbf{C}}, \quad \mathbf{C}_1 \le \mathbf{C}_2 \quad \text{and} \quad \mathbf{C}_c = \overline{\overline{\mathbf{C}}}, \quad \mathbf{C}_2 \le \mathbf{C}_1, \quad \text{(B.4f)}$$

$$\tilde{\mathbf{C}}' = 3\left[c_2\left(K_1 + \hat{K}_S\right) + c_1K_2 - K_c\right]\mathbf{H} + 2\left[c_2\left(\mu_1 + \hat{\mu}_S\right) + c_1\mu_2 - \mu_c\right]\mathbf{D} = 3\tilde{K}'\mathbf{H} + 2\tilde{\mu}'\mathbf{D}. \quad \text{(B.4g)}$$

Furthermore, as can be seen in Eq. (B.1), $\mathbf{H} + \mathbf{D} = \overset{4}{\mathbf{I}}$, so the rank four unit tensor, present in Eq. (4.14), can also be represented in the same form as all of the other tensors in that equations, specified earlier in this section. With that observation, the tensor of effective elastic constants $\mathbf{C}^*$ of Eq. (4.14) may be cast in the following form

$$\mathbf{C}^* = 3K^*\mathbf{H} + 2\mu^*\mathbf{D}, \quad \text{(B.5)}$$

and he remaining part of the Appendix is dedicated to development of formulas for the effective bulk modulus K^* and for the effective shear modulus μ^*.

The expression $\mathbf{L}:\tilde{\mathbf{C}}'$ in the right-hand side of Eq. (4.14) can be presented as follows

$$\mathbf{L}:\tilde{\mathbf{C}}' = \mathbf{L}:\left[3\left[c_2\left(K_1+\hat{K}_S\right)+c_1K_2-K_c\right]\mathbf{H}+2\left[c_2\left(\mu_1+\hat{\mu}_S\right)+c_1\mu_2-\mu_c\right]\mathbf{D}\right] =$$
$$= 9\,K\left[c_2\left(K_1+\hat{K}_S\right)+c_1K_2-K_c\right]\mathbf{H}+4b\left[c_2\left(\mu_1+\hat{\mu}_S\right)+c_1\mu_2-\mu_c\right]\mathbf{D}\,, \tag{B.6}$$

where $\hat{K}_S$ and $\hat{\mu}_S$, defined in (A.24a,c)

$$\hat{K}_S = \frac{4}{3R_0}\left[\lambda_S+\mu_S\right], \quad \hat{\mu}_S = \frac{1}{5R_0}\left[7\overline{\mu}_S+\overline{\lambda}_S\right]. \tag{B.7}$$

Then, the expression in the rightmost bracket of Eq. (4.14) can be transformed to the following form

$$c_2\mathbf{L}:\tilde{\mathbf{C}}_3 = \mathbf{L}:\left[c_2\mathbf{C}_3+3\hat{K}_S\mathbf{H}+2\hat{\mu}_S\mathbf{D}\right] =$$
$$= 9Kc_2\left[K_1+\hat{K}_S-K_2\right]\mathbf{H}+4bc_2\left[\mu_1+\hat{\mu}_S-\mu_2\right]\mathbf{D}\,. \tag{B.8}$$

Observing Eqs. (B.6), (B.8) and accounting for Eqs. (B.2)-(B.4) the formula for the tensor of effective elastic constants presented in Eq. (B.5) is arrived at, with the following scalar expression for the effective bulk and shear moduli

$$K^* = c_1\left[K_1+\hat{K}_S\right]+c_2K_2+\frac{9c_1c_2K\left[K_1-K_2+\hat{K}_S\right]^2}{1-9K\left[c_1K_2+c_2\left(K_1+\hat{K}_S\right)-K_c\right]}\,,$$

$$\mu^* = c_1\left[\mu_1+\hat{\mu}_S\right]+c_2\mu_2+\frac{4c_1c_2b\left[\mu_1-\mu_2+\hat{\mu}_S\right]^2}{1-4b\left[c_1\mu_2+c_2\left(\mu_1+\hat{\mu}_S\right)-\mu_c\right]}\,, \tag{B.9}$$

where K^* depends only on the K's defined in Eqs. (B.1) and (B.4), and μ^* depends only on μ's in those equations. K and $b(=\mu)$ of Eq. (B.4a) are further dependent on K_c and μ_c (in view of Eq. (4.7)) that are equal to either $\overline{K}$, $\overline{\mu}$ or $\overline{\overline{K}}$, $\overline{\overline{\mu}}$, depending on which of the conditions specified in Eq. (B.4f) is satisfied; $\hat{K}_S$ and $\hat{\mu}_S$ are defined in Eq. (B.7).

Acknowledgments

The first author gratefully acknowledges the financial support during May 3rd – May 17th , 2014, MTS Visiting Professor Appointment at the Department of Civil Engineering, University of Minnesota, Minneapolis, USA. Partial financial support by the German Research Foundation (DFG) via SFB 986 “M3" (project B6) is also gratefully acknowledged.

7. References

Brisard, S., Dormieux, L., Kondo, D., 2010. Hashin–Shtrikman bounds on the bulk modulus of a nanocomposite with spherical inhomogeneities and interface effects. Comput. Mater. Sci. 48 (3), 589–596.

Buryachenko, V.A., Roy, A., Lafdi, K., Anderson, K.L., Chellapilla, S., 2005. Multi-scale mechanics of nanocomposites including interface: Experimental and numerical investigation. Composites Science and Technology, 65, 2435–2465

Chen, T., Dvorak, G.J., Yu, C.C., 2007. Size-dependent elastic properties of unidirectional nano-composites with interface stresses. Acta Mechanica 188, 39–54.

Duan, H.L., Wang, J., Huang, Z.P., Karihaloo, B.L., 2005 Size-dependent effective elastic constants of solids containing nanoinhomogeneities with interface stress. J. Mech. Phys. Solids 53, 1574–1596.

Eshelby, J.D., 1957. The determination of the elastic fields of an ellipsoidal inclusions, and related problems. Proc. R. Soc. A 241, 376-396.

Gan, Y.X., 2009. Effect of interface structure on mechanical properties of advanced composite materials. Int. J. Mol. Sci., 10, 5115-5134.

Gibson, L.J., Ashby, M.F., 1988. Cellular Solids: structure and properties. Pergamon Press, Oxford.

Gurtin, M.E., Murdoch, A.I., 1975. A continuum theory of elastic material surfaces. Archive for Rational Mechanics and Analysis 57(4), 291–323.

Gurtin, M.E., Murdoch, A.I., 1978. Surface stress in solids. International Journal of Solids and Structures 14, 431–440.

Hashin, Z., Shtrikman, S., 1963. A variational approach to the theory of elastic behavior of multiphase materials. J. Mech. Phys. Solids 11, 127-140.

He, L.H., Li, Z.R., 2006. Impact of surface stress on stress concentration. International Journal Solids Structures 43, 6208–6219.

Huber, N, Viswanatha, R.N., Mameka, N., Markmanna, J., Weißmüller, J., 2014. Scaling laws of nanoporous metals under uniaxial compression. Acta Materialia, 67, 252-265.

Javili A., McBride A., Steinmann P., 2013. Thermomechanics of solids with lower-dimensional energetics: on the importance of surface, interface, and curve structures at the nanoscale. A Unifying Review, Applied Mechanics Reviews, 65, 010802-1.

Kanit, T., Forest, S., Galliet, I., Mounoury, V, Jeulin, D., 2003. Determination of the size of the representative volume element for random composites: statistical and numerical approach, Int. J. Solids Struct. 40, 3647–3679.

Khoroshun, L.P., 1978. Methods of random functions in determining the macroscopic properties of microheterogeneous media. Prikl. Mech. 14 (2), 113-124.

Khoroshun, L.P., Nazarenko, L.V., 1990. Thermoelasticity of orthotropic composites with ellipsoidal inclusions. International Applied Mechanics, 26 (9), 805 - 812.

Khoroshun, L.P., Nazarenko, L.V., 1992. Effective elastic properties of composites with disoriented anisotropic ellipsoidal inclusions. Int. Applied Mechanics 28 (12), 801 – 808.

Khoroshun, L.P., Maslov, B.P., Shikula, E.N., Nazarenko, L.V., 1993. Statistical Mechanics and Effective Properties of Materials, Naukova dumka, Kiev [in Russian].

Kickelbick, G., 2007, Hybrid Materials Synthesis, Characterization, and Applications, WILEY-VCH Verlag GmbH & Co. KGaA, Weinheim.

Kim, J.K., Mai, Y.W., 1998. Engineered interfaces in fiber reinforced composites. New York: Elsevier.

Kushch, V.I., Mogilevskaya, S.G., Stolarski, H.K., Crouch, S.L., 2013. Elastic fields and effective moduli of particulate nanocomposites with the Gurtin–Murdoch model of interfaces. International Journal of Solids and Structures 50, 1141–1153.

Lim, C.W., Li, Z.R., He, L.H., 2006. Size-dependent, non-uniform elastic field inside a nano-scale spherical inclusion due to interface stress. International Journal of Solids and Structures 43, 5055–5065.

Ma, P.C., Kim, J.K., 2011. Carbon Nanotubes for Polymer Reinforcement, Taylor and Francis Group.

McBride, A.T., Javili, A., Steinmann, P., Bargmann, S., 2011. Geometrically nonlinear continuum thermomechanics with surface energies coupled to diffusion. J. Mech. Phys. Solids 59, 2116–2133.

McBride, A.T., Mergheim, J., Javili, A., Steinmann, P., Bargmann, S., 2012. Micro-to-macro transitions for heterogeneous material layers accounting for in-plane stretch. J. Mech. Phys. Solids 60, 1221–1239.

Miller, R.E., Shenoy, V.B., 2000. Size-dependent elastic properties of nanosized structural elements. Nanotechnology 11, 139–147.

Mogilevskaya, S.G., Crouch, S.L., Grotta, A.L., Stolarski, H.K., 2010a. The effects of surface elasticity and surface tension on the transverse overall elastic behavior of unidirectional nano-composites. Composites Science and Technology 70, 427–434.

Mogilevskaya, S.G., Crouch, S.L., Stolarski, H.K., Benusiglio, A., 2010b. Equivalent inhomogeneity method for evaluating the effective elastic properties of unidirectional multiphase composites with surface/interface effects. International Journal of Solids and Structures 47, 407–418.

Mura, T., 1987. Micromechanics of Defects in Solids, Martinus Nijhoff Publishers, Dortrecht, The Netherlands.

Nazarenko, L., Khoroshun, L., Müller, W.H., Wille, R., 2009. Effective thermoelastic properties of discrete-fiber reinforced materials with transversally-isotropic components. Continuum mechanics and thermodynamics 20, 429-458.

Nazarenko, L., Bargmann, S., Stolarski, H.. 2014. Influence of interfaces on effective properties of nanomaterials with stochastically distributed spherical inclusions. International Journal of Solids and Structures 51, 985-997.

Roberts, A.P., Garboczi, E.J., 2002. Elastic properties of model random three-dimensional open-cell solids J. Mech. Phys. Solids 50, 33 – 55.

Sarac, B., Wilmers, J., Bargmann, S., 2014. Property optimization of metallic glasses via structural design. Materials Letters, accepted for publication.

Sharma, P., Ganti, S., 2004. Size-dependent Eshelby's tensor for embedded nanoinclusions incorporating surface/interface energies. Journal of Applied Mechanics 71, 663–671.

Shenoy, V.B., 2005. Atomistic calculations of elastic properties of metallic fcc crystal surfaces. Physical Rev. B71, 094104.

Wang, K.,Weissmüller, J, 2013. Composites of Nanoporous Gold and Polymer. Adv. Mater., 2013, 25, 1280–1284

Willis, J.R., 1977. Bounds and self-consistent estimates for the overall properties of anisotropic composites. J. Mech. Phys. Solids **25** (2), 185-202.

Yang, F.Q., 2004. Size-dependent effective modulus of elastic composite materials: spherical nanocavities at dilute concentrations. Journal of Applied Physics 95, 3516–3520.